

Reproduction Quality Notice

This document is part of the Air Technical Index [ATI] collection. The ATI collection is over 50 years old and was imaged from roll film. The collection has deteriorated over time and is in poor condition. DTIC has reproduced the best available copy utilizing the most current imaging technology. ATI documents that are partially legible have been included in the DTIC collection due to their historical value.

If you are dissatisfied with this document, please feel free to contact our Directorate of User Services at [703] 767-9066/9068 or DSN 427-9066/9068.

**Do Not Return This Document
To DTIC**

Reproduced by
AIR DOCUMENTS DIVISION



HEADQUARTERS AIR MATERIEL COMMAND

WRIGHT FIELD, DAYTON, OHIO

The
U.S. GOVERNMENT

IS ABSOLVED

FROM ANY LITIGATION WHICH MAY

ENSUE FROM THE CONTRACTORS IN -

FRINGING ON THE FOREIGN PATENT

RIGHTS WHICH MAY BE INVOLVED.

REEL - C

1 3 2

A.T.I.

5 5 3 6

AFR Jan. 1943

NATIONAL ADVISORY COMMITTEE FOR AERONAUTICS

ATI No. **5536**

WARTIME REPORT

ORIGINALLY ISSUED
January 1943 as
Advance Restricted Report

FLIGHT INVESTIGATION OF NACA D₃ COWLINGS ON THE
XP-42 AIRPLANE. I - HIGH-INLET-VELOCITY
COWLING WITH PROPELLER CUFFS TESTED
IN HIGH-SPEED LEVEL FLIGHT

By F. J. Bailey, Jr., and J. Ford Johnston

Langley Memorial Aeronautical Laboratory
Langley Field, Va.

AIR DOCUMENTS DIVISION, T-2
AMC, WRIGHT FIELD
MICROFILM NO.
RC-132 F 5536



NACA

WASHINGTON

RECEIVED
JUN 30 1947

NACA WARTIME REPORTS are reprints of papers originally issued to provide rapid distribution of advance research results to an authorized group requiring them for the war effort. They were previously held under a security status but are now unclassified. Some of these reports were not technically edited. All have been reproduced without change in order to expedite general distribution.

NATIONAL ADVISORY COMMITTEE FOR AERONAUTICS

ADVANCE RESTRICTED REPORT

FLIGHT INVESTIGATION OF NACA D₈ COWLINGS ON THE
XP-42 AIRPLANE. I - HIGH-INLET-VELOCITY
COWLING WITH PROPELLER CUFFS TESTED
IN HIGH-SPEED LEVEL FLIGHT

By F. J. Bailey, Jr., and J. Ford Johnston

SUMMARY

Results are presented of a series of flight tests of the maximum speed and cooling characteristics in full-throttle level flight of the XP-42 airplane equipped with a short-nose high-inlet-velocity cowling. This cowling is one of a series being tested in an effort to improve the performance and cooling characteristics of air-cooled engine installations.

The results of the tests indicated a maximum speed of 336 miles per hour at 960 horsepower at 15,000 feet.

Pressure measurements in the entrances to the cylinder baffles showed a fairly uniform distribution of pressure around the engine at similar points of measurement on individual cylinders but indicated that cooling-air pressures varied considerably for different points of measurement on the same cylinder. The variation was probably due to the velocity head of the entering cooling-air jet. Static pressure behind the engine was uniform.

Front pressures on the engine averaged 80 percent and rear pressures 59 percent of free-stream impact pressure. The resulting pressure drop of 15 inches of water at full throttle at 15,000 feet cooled the cylinder heads adequately; maximum cylinder base temperatures, however, exceeded the specified limits when corrected to Army summer conditions.

Pressure measurements in the carburetor and oil-cooler ducts showed rams of slightly over 100 percent of free-stream impact pressure. Air-flow measurements in the car-

buret duct and in the annular entrance to the engine compartment showed that the volume flows of induction and cooling air were approximately constant at full throttle over a range of altitudes near the critical altitude and were, respectively, 2960 and 19,900 cubic feet of free air per minute.

INTRODUCTION

The National Advisory Committee for Aeronautics is investigating means of modifying the conventional NACA radial engine cowling to meet the demands imposed by the latest designs of military airplanes. Tests in a number of the wind tunnels have been directed toward improving the cowlings in the following respects:

1. Greater stability of the air flow within the cowlings, particularly at angles of attack corresponding to the climb condition, to provide a uniform cooling-air pressure in front of the engine
2. Reduction of energy losses in the cooling air in front of the engine by the use of an efficient diffuser between the inlet and the front face of engine
3. Adequate ground cooling characteristics
4. Improvement in the external shape to reduce drag and to increase the critical speed of the cowlings

The NACA D-series cowlings have been developed to meet these requirements. The D cowlings are characterized by the use of a cowlings inner liner and of an afterbody behind the spinner. These units form an annular entrance followed by a diffuser section made up of the afterbody and inner liner. Investigations such as reported in references 1 and 2 have indicated desirable ranges of cooling-air inlet velocities, diffuser proportions, and external contours.

In order to expedite incorporation of these new features in projected designs for military aircraft, the NACA is conducting flight tests of the Curtiss XP-42 airplane fitted with several engine installations utilizing the latest developments of the NACA cowlings and individual cowlings jet exhaust stacks (reference 3).

The XP-42 airplane is powered by a Pratt & Whitney 1930-31 engine. As originally furnished with the airplane, this engine carried an extension shaft that placed the propeller 20 inches ahead of the normal position. The first of the cowlings included in the series of tests was designed for this long-nose engine and represented a complete redesign of the cowling furnished with the airplane. The development of this cowling in the full-scale wind tunnel is described in reference 2 and the flight-test results are presented in reference 4.

The present report is the first of a series of reports on the short-nose (D_3) cowlings and contains the results of tests in the high-speed level-flight condition of the high-inlet-velocity cowling, which was designed for the short-nose Pratt & Whitney 1830 engine. This cowling was tested on the XP-42 airplane by replacing the nose-extension shaft of the 1930-31 engine with a shaft of standard size.

For convenience, test numbers have been assigned each cowling arrangement and flight condition. Tests 1 and 2 were the high-speed and climb tests of the long-nose cowling and test 3 is the investigation on the short-nose cowling reported herein. Further identification has been given by prefixing this test number to the number for a particular flight, which was arbitrarily assigned. For example, flight 3-6 indicates flight 6 in which the airplane was in test condition 3.

It was necessary to defer the final part of the tests of this cowling, involving determination of its cooling characteristics in climb, until the scheduled high-speed tests of other arrangements had been completed and the inadequate cowl flap installation could be modified as in reference 4.

The design of the cowling and engine installation was a project of the Air-Cooled Engine-Installation Group stationed at the Laboratory. The members of the group associated with this project included Mr. Howard S. Ditch, of the Curtiss Wright Corporation; Mr. Peter Terraco, of the Republic Aviation Corporation; Mr. William S. Richards, of the Wright Aeronautical Corporation; and Mr. James R. Thompson, of Pratt & Whitney Aircraft. The Materiel Command, Army Air Force sponsored the investigation and supplied the XP-42 airplane. The Airplane Division of the Curtiss-Wright Corporation handled the construction as

well as the structural and detail design of the cowling, and supplied personnel to assist in the servicing and maintenance of the airplane and cowling during the tests. Pratt & Whitney Aircraft prepared the engine and torque meter for the tests and assisted in the operation and servicing of the engine. The propeller, cuffs, and spinner were supplied by the Propeller Division of the Curtiss-Wright Corporation.

This report was originally issued as a memorandum report for the Army Air Corps.

XP-42 AIRPLANE WITH SHORT-NOSE COWLING

The XP-42 airplane is identical with the P-36 airplane except for the fuselage fairing behind the cowling and the installation of its Pratt & Whitney 1830 engine with its higher critical altitude rating. The power rating of the engine is as follows:

	Brake horsepower	Engine speed (rpm)	Altitude (ft)
Take-off	1050	2550	0
Normal rating	1000	2300	8,500
Normal rating	1000	2450	11,500
Military rating	1000	2700	14,500

The engine has a single-stage blower with an impeller-drive ratio of 8.47:1 and a propeller-drive ratio of 9:16. The engine-cylinder baffles were reworked to minimize the leakage of air between adjoining baffles and to direct the cooling air on the cylinders in an efficient manner.

The 10-inch-diameter oil cooler furnished with the engine was replaced by an 11-inch U.A.P. cooler with the same core depth of 9 inches. Individual jet exhaust stacks were used in place of the standard collector ring. These stacks are made of 0.049-inch stainless-steel tubing of $2\frac{3}{8}$ -inch outside diameter. The ends of the stacks were flattened to reduce the internal area from 4.05 to 2.98 square inches.

5

The engine cowling and propeller cuffs were fabricated by the Curtiss-Wright Corporation and are shown in figures 1 to 6.

The fuselage side panels reported in references 1 and 2 were used to improve the fairing of the cowling into the fuselage. The airplane, as prepared for the tests, weighed about 6000 pounds with 175-pound pilot and full tanks. It retained the standard aerial, but had no provisions for guns.

TEST APPARATUS

The installation of test equipment was designed to give as nearly as possible a continuous record of the pertinent data, with the exception of air-flow measurements, throughout each flight. Continuous records were taken of airspeed, altitude, manifold pressure, engine speed and torque, and temperatures. Air flows were measured by recording instruments during the particular flight conditions under investigation.

Free-stream impact pressure was measured by an NACA airspeed recorder connected to an airspeed boom on the right wing tip (fig. 7). The boom carried a fixed static head about one chord length ahead of the leading edge of the wing and a special shielded impact head halfway between the static head and the leading edge of the wing. The static head was calibrated in flight by flying at a known geometric height at several airspeeds with a sensitive altimeter (fig. 8) connected to the static head. The shielded impact head is accurate at all angles of attack encountered in steady flight.

Atmospheric pressure was measured by an NACA recording altimeter vented to the compartment behind the cockpit in which the recording instruments were installed. Pressure data so acquired were corrected for the measured difference between the compartment pressure and true static pressure.

In the same instrument was incorporated another cell that recorded absolute manifold pressure at the supercharger blower rim.

The pressure from a Pratt & Whitney oil-pressure torque meter installed in the nose of the engine was trans-

mitted both to a gage in the pilot's cockpit and to an NACA pressure recorder having a range of 400 pounds per square inch. This installation permitted both visual and recorded indications of the torque delivered to the propeller. This record, in conjunction with the engine-speed record, permitted calculation of the brake horsepower delivered to the propeller at any time during the flight.

Engine speed was recorded by means of a revolution counter took off the tachometer drive. At every 200th revolution of the engine, a contact was made that operated a solenoid and made a mark on the airspeed film. Since a chronometric timer was also used to mark the film every 3 seconds, the time for 200 revolutions could be calculated from the relative distances along the film of engine speed and timer marks.

All temperature records were made by means of thermocouples connected through two 34-position rotating switches to a two-coil recording galvanometer. The cold junctions of all thermocouples were placed in pans surrounded by an ice-and-water bath to keep them at constant temperature. The leads to the cold-junction box are shown in figure 9. The box containing the ice-and-water bath is concealed by the felt wrapping used to insulate the bath from the cockpit temperatures. The switch speed was such that each temperature was recorded about once every 45 seconds.

All cylinder-head and barrel temperatures were measured, the heads by means of gasket-type thermocouples under the rear spark plugs, and the barrels by means of thermocouples peened into the flanges at the rear center line. Other temperature recordings included:

- Intake mixture at intake ports of cylinders 5 and 10
- Front and rear spark-plug elbows of cylinders 1, 7, and 11
- Right and left magnetos
- Fuel on suction and pressure sides of pump and in carburetor float chamber
- Mixture at supercharger blower rim

Oil out

Oil-in line

Free air (under left wing outside slipstream, see figs. 10 and 11)

Air just ahead of screen in carburetor scoop

Air at entrance to engine compartment

Engine cooling air ahead of cylinder 1 and between cylinders 2 and 14

Engine cooling air 2 inches behind cylinder 1 and three fin spaces above bottom of head

Air at exit from oil cooler

Accessory compartment

Pilot's cockpit

Recording instrument compartment

An additional thermocouple was placed in a thermos bottle (fig. 12) containing hot ethylene glycol, the temperature of which was checked with a mercury thermometer just before take-off and just after landing.

Engine cooling, carburetor and oil-cooler air flow, as well as several additional pressure measurements, were made by means of an NACA multiple recording manometer in conjunction with twelve 9-position rotating pressure switches, which made possible the recording of 108 different pressures within about 30 seconds. The installation of the manometer and switches is shown in figures 13 and 14.

For the measurement of engine cooling-air flow, three pressure rakes were set 120° apart in the annular entrance to the engine compartment. Each rake consisted of five impact tubes spaced radially across the opening and one static tube about 1 inch to the side of the center impact tube. Figure 15 shows the right and left rakes.

The pressure at the entrance to the cylinder baffles was measured by a total of 37 impact tubes distributed

between cylinders 1, 3, 4, 6, 7, 9, 10, 12, and 14. Each of these cylinders carried two impact tubes on the exhaust side of the cylinder, one about three fin spaces below and the other about three fin spaces above the bottom of the head; a third tube was in the fins on top of the cylinder head. In addition, cylinders 1, 6, and 10 had impact tubes similarly located on the intake sides of the heads and barrels and cylinders 3 and 4 carried tubes between the top-most concentric head fins and between the lowest barrel fine on the exhaust sides of the cylinders. Some of the tubes in the baffles of cylinders 9 and 10 are indicated by arrows in figure 16. The pressure rake shown was installed after completion of the tests reported herein and preparatory to tests of a blower-cooled installation. Static pressure behind the engine cylinders was measured by open-end tubes sheltered from direct air flow behind and just below each of the nine cylinders on which the impact tubes were placed.

The air flow and the ram to the carburetor were determined by means of a rake (see fig. 17) of five impact tubes on the vertical center line of the scoop about 2 inches behind the center line of the rear cylinders and three static tubes about 1 inch to the side of the impact tubes. Holes flush with the top and bottom walls of the duct gave the static pressure in the boundary layer. Connections were also made to the carburetor impact-pressure tubes below the screen and to the pressure in the float chamber, beyond the altitude compensator.

Pressures in front of the oil cooler (fig. 18) were measured by means of three impact and three static tubes disposed along the vertical center line of the oil cooler, their openings being about $\frac{3}{4}$ inches in front of the face of the oil cooler. Three impact tubes were placed about $\frac{1}{2}$ inch behind the rear face of the oil cooler, also on the vertical center line, and a shielded impact tube accurate to about 20° of yaw was set in the exit air stream at the trailing edge of the oil-cooler flap (fig. 19). The relative locations of points of pressure measurement are indicated in figures 6 and 20.

Additional pressure measurements include accessory-compartment, recording-instrument-compartment, and pilot's-cockpit pressures, as well as free-stream impact pressure.

All impact and static tubes to the manometer were of

$\frac{1}{8}$ -inch copper tubing, 0.06-inch inside diameter, with leads not less than 12 nor more than 15 feet long.

L-383

Instrument readings made by the pilot included oil-in, carburetor-mixture, and free-air temperatures from vapor-pressure thermometers already installed in the airplane. For the last two flights, a resistance-bulb thermometer with a ratio-type indicator was installed in place of the vapor-pressure free-air thermometer. All free-air thermometers were calibrated for the heating effect due to speed by flying at constant altitude at several airspeeds. The calibrations are shown in figure 21. It was decided that the free-air temperatures recorded by the thermocouple were the most reliable, and these free-air temperatures, corrected for compressibility, are used in this report.

Attempts were made to measure the fuel flow to the engine by two separate methods. One method was by the use of an NACA recording flowmeter installed in the fuel line between the pump and the carburetor; the other was by measuring the pressure drops across the main and economizer jets in the carburetor, which had been calibrated previously on the flow bench. Analysis of the data subsequent to the tests indicated that neither method gave satisfactory results as installed, and no fuel-flow data are presented in this report. It is thought, however, that further development will result in making one or both of these methods of fuel-flow measurement satisfactory and may permit reclamation of the data obtained in these tests.

TEST PROCEDURE

Because the cowling was equipped with only enough cowl-flap area to cool the engine in a medium climb, all full-power testing was confined to the high-speed level-flight condition. The flight tests, then, fell into three groups: first, preliminary ground tests and flights at increasing altitudes and powers to make sure that cooling at full power and critical altitude would be within the allowable limits and to calibrate the airspeed head and free-air thermometer; second, full-power level flights with the original cuffs at several altitudes at and above the engine critical altitude (flights 3-6, 3-8, and 3-9); and third, full-power level flights at approximately the same altitudes as in the second group, but with the cuff angles reduced by about 2° (flights 3-10 and 3-11).

The typical procedure used for testing high speed and cooling pressures may be seen from an inspection of the time histories of the flights (figs. 22, 23, and 24). The pilot made a gentle climb to approximately the rated critical altitude of the engine (14,500 ft), then leveled out, closed the cowl flaps, and went to full throttle at 2700 rpm in the automatic-rich carburetor setting. After reaching constant speed, the pilot switched on the manometer and fuel flowmeter for about 40 seconds, or for slightly more than one cycle of the rotating pressure switches. (All other recording instruments were left on from take-off to landing.) The interval thus covered was considered to be the "run" for purposes of determining the high-speed and cooling characteristics of the airplane at that altitude and power. Upon completion of the run, the pilot would climb to the next altitude (usually about 800 ft higher) and make another run of the same type. In each of the flights for high speed, runs were made at four altitudes. For the last flight with the modified cuffs, one high-speed run was made at an indicated altitude of 17,000 feet in automatic rich, after which the carburetor-mixture control was changed to full rich and then leaned out progressively in order to find whether a higher power could be attained with a different mixture. When the mixture was changed from automatic rich to full rich, the torque dropped 13 percent at constant engine speed; when the mixture was leaned, the torque rose but started to fall off again after almost reaching the value obtained in the automatic rich setting. As it was not considered safe to lean the mixtures below the point at which the torque started to fall off, the pilot immediately set the mixture control back to automatic rich and ended the experiment. A subsequent study of the relative fuel-flow data indicated, however, that the rate of fuel flow to the engine during manual mixture control was never as low as the rate of fuel flow in automatic rich; the unexplored region was indicated to be of the order of 70 pounds of gasoline per hour. The fuel-flow records also indicated that the mixture was becoming slightly richer, rather than leaner, during the last part of the period of manual control.

RESULTS

In figures 22, 23, and 24 are presented time histories of the main high-speed flights, giving the recorded pressure altitude; indicated airspeed; manifold pressure;

torque; engine speed; and head, barrel, and other selected temperatures during the flight. The brake horsepower as calculated from the torque and engine-speed curves is also given.

The periods of steady level flight at different altitudes during which the high speed was being measured are indicated on the time histories. The data pertinent to the determination of maximum speed that were recorded during these runs are plotted to an enlarged scale in figure 25. The values of maximum speed and power calculated from these data for each run are given in table I along with simultaneously recorded data on engine temperatures and cooling and induction air pressures.

DISCUSSION

Maximum Speed

The values of maximum speed given for each run in table I were computed from values of impact and static pressure selected, after inspection of the enlarged time histories of figure 25, as being most representative of steady level flight. Comparison of the values for all runs over the altitude range covered shows a maximum spread of approximately 5 miles per hour in speed. The faired curve of speed against altitude in figure 26 suggests that about 20 percent of this spread is attributable to a consistent variation of speed with altitude. The remaining spread of approximately 4 miles per hour indicates the consistency with which the maximum speed values could be reproduced in different runs under different atmospheric conditions.

The relation between the observed variations of power and speed with altitude shown in figure 26 is most easily understood by consideration of the equilibrium of power required and power available in steady level flight. Under these conditions

$$\frac{DV}{575} = \eta \text{ bhp} \quad (1)$$

or

$$V = 52.73 \left(\frac{\eta}{SC_D} \right)^{1/3} \left(\frac{\text{bhp}}{\sigma} \right)^{1/3} \quad (2)$$

where

D over-all drag of airplane, pounds
 V true airspeed, miles per hour
 η propulsive efficiency of propeller and exhaust stack combination
 bhp brake horsepower
 S wing area, square feet
 C_D drag coefficient of airplane
 σ density ratio

It is immediately apparent that, for full-throttle level flight at and slightly above the critical altitude of an airplane of normal aspect ratio and wing loading and a propeller chosen for good high-speed performance,

the value of the parameter $53.73 \left(\frac{\eta}{SC_D} \right)^{1/3}$ should be virtually unaffected by moderate changes in weight or altitude. Values of this parameter deduced from the observed values of V and $\frac{bhp}{\sigma}$ for each run are plotted against density altitude in figure 27. As expected, little variation with altitude is apparent.

Under the conditions just described, the parameter

$\left(\frac{bhp}{\sigma} \right)^{1/3}$ would also be expected to remain essentially constant over the altitude range covered by the tests. The measured values of this parameter, which are also plotted against density altitude in figure 27, confirm this expectation.

One important phase of the present investigation involves comparison of the high-speed performance of the short-nose cowl and exhaust stack arrangement with that of a similar long-nose version tested previously on the same airplane (reference 4). It has also been suggested that the results might be compared with accepted high-speed performance results for similar airplanes with conventional air-cooled (P-36A) and liquid-cooled (P-40C) in-

installations. In order to provide such a comparison, equation (2) in the modified form

$$\left(\frac{V}{52.73}\right)^3 = \left(\frac{\eta}{SC_D}\right) \left(\frac{bhp}{\sigma}\right) \quad (3)$$

is presented graphically in figure 28. Points representing the high-speed performance of the various airplanes, all of which have the same wing area, are spotted in this figure. The location of a point on the figure immediately reveals not only the maximum speed of the airplane but also the manner by which that speed is attained; that is, by power, supercharging, and ram as indicated by the ordinate scale, or by aerodynamic refinement, as indicated by the abscissa scale.

Within reasonable limits, the figure may be used for several purposes. Primarily, it provides a ready method for determining the effect on maximum speed of changing the critical altitude of an engine installation by either supercharging or ram, or by reducing preheating of the carburetor air. When the corresponding changes in the weight and the propulsive efficiency are small, the effect on the factor $\frac{\eta}{SC_D}$ will be negligible. The abscissa of a point on the figure may therefore be assumed to remain constant while the ordinate is shifted. For instance, for purposes of comparing the cleanness of the two installations in terms of speed at the same horsepower and altitude, it might be assumed that the induction system of the long-nose XP-42 could be modified without increase in drag to get the same high ram as obtained with the short-nose XP-42. In that case, as the same engine was used in both installations, the observed points for the long nose would be shifted upward to the same average value of $\frac{bhp}{\sigma}$ as was observed for the short nose; and the long-nose installation would be expected to attain a maximum speed of 341 miles per hour, compared with the observed maximum speeds of 336 miles per hour for the short nose and 338 miles per hour for the long nose. The chart shows then that the cleanness of the long-nose installation is not fully exploited because of losses in the induction system.

The comparison may be extended to include the P-36A and P-40C, with limitations to be noted later. Inasmuch as the engines of all these airplanes have been rated at

1050 horsepower at various altitudes, it may be assumed that the radial engines could be supercharged to 1050 horsepower at 15,000 feet, or, in other words, to the same power and altitude as that of the P-40C. The comparison would then show:

Airplane	Observed maximum speed (mph)	Maximum speed at 1050 hp at 15,000 ft (mph)
P-40C	347	347
XP-42 long nose	338	352
XP-42 short nose	336	347
P-36A	313	335

This comparison is subject to certain limitations. The engine powers of the P-36A and P-40C were not measured by an engine torque meter and are therefore open to some question. Some additional cooling power would be required to cool the P-36A and the XP-42 engines to the same power rating as the P-40C engine. Comparison of the aerodynamic effect of the engine installation is further complicated by the fact that other sources of drag are not strictly comparable because the gun installations on the XP-42 had been removed and because, on the other hand, some detailed aerodynamic refinements, such as the landing-gear fairing, have been made on the P-40C.

The comparison, however, does appear to indicate that, by use of individual jet exhaust stacks and a high-inlet-velocity cowling, the installation of an air-cooled engine may be made to compare favorably with a conventional liquid-cooled engine installation.

Pressures and Temperatures

The variation of cylinder temperatures around an engine is influenced by a number of factors, such as non-uniform charge and mixture distribution, that are in no way a function of the cowling design. Unless the effect of these factors can be determined, the merit of a cowling designed for general application cannot be reliably

L-383

evaluated by measurements of engine temperatures alone on a specific application. For this reason, primary emphasis in the present tests has been centered on determining the extent to which the type of cowling under consideration provides a high, uniformly distributed pressure over the front of the engine and a suitable, uniformly distributed pressure over the rear of the engine.

Figures 29 to 31 present the results of the pressure and temperature measurements in a graphical form that shows the distribution of both pressure and temperature around the engine for several typical runs. These data indicate that, while pressures at the baffle entrances vary somewhat with the location of the cylinders on which they are measured, they vary even more critically with the point of measurement on the individual cylinder. Values, averaged around the engine, of the front pressures recorded at particular locations in the cylinder baffles are given in table II. They indicate a deficiency of front pressure at the top of the heads of the front cylinders and at the bottom of the barrels of both front and rear cylinders.

In the type of cowling under consideration, in which cooling air is introduced to the engine compartment through a fairly narrow annular opening, the front pressures on the engine, and particularly on the front cylinders, may be expected to vary up and down the cylinder with respect to the location of the entering jet, the magnitude of the variation depending upon the velocity of the jet and the distance of the cylinder behind the jet. If space permits the use of a well-designed diffuser section in the annulus, the jet entering the engine compartment will have negligible velocity head and turbulent losses will also be negligible. The result should then be a high uniform pressure on the front of the engine, the pressure being equal to that in the annulus. If such a diffuser is not or cannot be used, it may reasonably be expected that the maximum variation of front pressures will not exceed the difference between the impact pressure and static pressure of the air at the exit from the diffuser, or, the velocity head of the jet. It is interesting to note in this connection that the lowest pressures measured in the baffles were approximately equal to the measured static pressure in the annulus and that none of the front pressures were as high as the impact pressure in the annulus. The average pressure on the front of the engine was approximately $0.13q_c$ lower than the average impact pressure in the annulus (q_c , airplane impact press.).

The general trend of pressure distribution around the engine indicates that the highest front pressures occurred on the bottom of the engine; whereas the lowest front pressures occurred on the right and the left upper sides of the engine. When average pressures over all high-speed runs are plotted for each common point of pressure measurement, as in figure 32, it is seen that the only points following this trend are the pressures on top of the heads. With the exception of cylinder 3, the distribution of pressure on the side of the heads and barrels was uniform around the engine. The pressure tubes on the side of cylinder 3 were directly behind a large ignition-cable conduit and probably lay in its wake. Although there were usually other obstructions, such as push rods and ignition cables, in front of the other pressure tubes, none were so large as the conduit. These obstructions, however, may account for some of the observed difference in total pressure between the annulus and the engine.

Individual cylinder temperatures showed little tendency to correlate with the pressure drops across the individual cylinders. It may be noted in particular that, although pressures over the top of the front cylinder heads were lower than those over the top of the rear heads, the front head temperatures were lower than those of the rear heads. In this case, the observed pressures on top of the front heads may provide erroneous indications of the air flow, because the tops of the fins, where the pressure tubes were located, were above the direct air jet but the lower halves of the fins were exposed to the jet from the annulus. (See fig. 6.)

An inspection of the cylinder temperatures around the engine shows that the right side of the engine was cooler than the left. The left cylinder heads were on the average, about 35° F hotter than the right, and the left cylinder bases were correspondingly about 10° F hotter than the right. The front base temperatures were slightly higher than the rear base temperatures. There is no apparent explanation why the left side of the engine was hotter than the right, because front and rear cooling-air pressures were nearly uniform.

In figure 33 average head and barrel temperatures in °F above free-air temperature are plotted, along with the cooling-air pressure drops, averaged over the engine, for full-throttle operation over a range of density altitudes above the critical. Also shown are the brake horsepower

and manifold pressures. The change from the original cuffs (flights 3-8 and 3-9) to the modified cuffs (flight 3-10) produced little apparent change in any of the quantities shown. Although individual pressures and temperatures showed little correlation, the variation of average pressures and temperatures was consistent.

A considerable rise in cylinder temperatures at altitudes above critical altitude appears to have resulted from the net effect of decreasing power and decreasing pressure drop. An important probable factor in this temperature rise, however, was the decrease in fuel-air ratio as the manifold pressure decreased at altitudes above the critical altitude. The power compensation of this carburetor depends upon the manifold pressure.

The recommended limiting temperatures for the engine used in these tests were 500° F for the cylinder heads and 335° F for the barrels at the points of measurement used. Army specifications require that the installation be capable of operating within these limiting temperatures under "summer conditions," that is, sea-level temperature is 100° F and the variation of temperature with pressure altitude is 3.6° F per 1000 feet. For correcting tests to these air conditions, a 1:1 temperature correction factor is specified for both heads and barrels. Figure 34 shows the observed head and barrel temperatures in relation to these Army limits. It is immediately apparent that, although head temperatures were relatively low, the maximum barrel temperatures exceeded the Army limits at and above critical altitude even though the engine was operating below its rated military power. A redistribution of available cooling air to provide more pressure at the base of the cylinders would probably correct this condition.*

Figure 35 presents a comparison of the average pressures available at several locations in the cowling. The highest pressures were observed in the carburetor duct,

*Subsequent tests on the same engine and thermocouple installation in another short-nose cowling showed that a reduction of 15° F in the temperature of the base thermocouples could be obtained by removal of the baffle sealing strips between the barrels at the bottom of the cylinders. The sealing strips are a special feature of the particular baffle arrangement provided by Pratt & Whitney Aircraft for the engine used in this investigation and are not present in the standard baffle installation for 1850 engines.

where the average pressure was about 104 percent of free-stream impact pressure. This result indicated that the cuffs were loaded even in the high-speed condition. The difference in average pressure between the carburetor duct and the annulus is largely chargeable to the boundary-layer effect on the spinner; whereas the difference between the annulus and the front of the engine, as has been noted, was probably caused by turbulent losses in the rapid expansion from the annulus to the engine compartment. The large boundary-layer effect on the inner edge of the annulus, which forms a continuation of the spinner, may be observed in figure 36, which shows the average pressure distribution in the annulus and in the carburetor duct. The data in table I on impact and static pressures at the surveys in the annular entrance to the engine compartment indicate that the ratio of the velocity head at any point in the survey plane to free-stream impact pressure remained essentially constant over the range of power, altitude, and angle-of-attack conditions covered during the full-throttle high-speed runs. From the faired curves of the ratio of impact and static pressures to free-stream impact pressure, averaged for all three surveys and all high-speed runs as shown in figure 36, it has been found that

$$\int_{\text{inner wall}}^{\text{outer wall}} \sqrt{\frac{\frac{1}{2} \rho_s V_s^2}{q_c}} dA = 0.640$$

where

- $\frac{1}{2} \rho_s V_s^2$ dynamic pressure at surveys, pounds per square foot
- q_c airplane impact pressure, pounds per square foot
- A area of annular entrance at survey, square feet
- ρ_s air density at survey plane, slugs per cubic foot
- V_s air velocity at survey plane, feet per second

The mass flow of air to the engine is

$$\rho_s V_s A = 0.640 \sqrt{2 \rho_s q_c}$$

The volume flow of free air at density ρ_{fa} is

$$\frac{\rho_{s-g} V A}{\rho_{fa}} = 0.640 \sqrt{\frac{2 \rho_{s-g} q_c}{\rho_{fa}}}$$

Temperature and pressure measurements at the surveys indicate that the density at the surveys ranged from 4 to 6 percent above free-air density so that

$$\text{Volume flow} = 0.938 \sqrt{\frac{q_c}{\rho_{fa}}}$$

Inspection of figure 35 shows that, within the limits of experimental error, the value of $\sqrt{\frac{q_c}{\rho_{fa}}}$ may be taken as

357 at all altitudes covered by the tests. Hence, the flow of cooling air to the engine was 331 cubic feet of free air per second, or 19,860 cubic feet of free air per minute.

Evaluated in a similar manner, the data for the flow in the carburetor duct indicates that

$$\text{Volume flow} = 0.138 \sqrt{\frac{q_c}{\rho_{fa}}} \text{ cubic feet per second}$$

$$= 2960 \text{ cubic feet of free air per minute}$$

Inasmuch as the ratio of horsepower to density was constant, this result leads to the conclusion that the specific air consumption was also nearly constant at 8.9 pounds per brake horsepower-hour.

CONCLUSIONS

Results have been given of high-speed level-flight tests of a short-nose high-inlet-velocity cowling with propeller cuffs on the XP-43 airplane. These results are intended for use in comparisons with other cowlings tested on the same airplane, and for this reason the data obtained have been fully presented.

1. The observed airplane maximum speed was 336 miles per hour at 960 horsepower at 15,000 feet density altitude.

2. Cooling-air pressure recovery on the front of the engine averaged about 80 percent of free-stream impact pressure. The pressure distribution was fairly uniform.

3. With 15 inches of water pressure drop across the engine, the cylinder head temperatures were relatively low, but cylinder base temperatures were slightly above their Army limit.

Langley Memorial Aeronautical Laboratory,
National Advisory Committee for Aeronautics,
Langley Field, Va.

REFERENCES

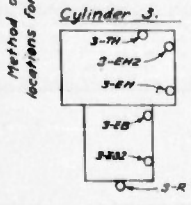
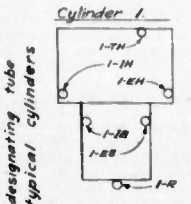
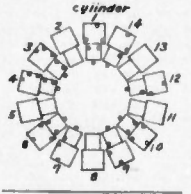
1. Valentine, E. Floyd: Preliminary Investigation Directed toward Improvement of the NACA Cowling. NACA A.R.R., April 1942.
2. Silverstein, Abe, and Guryansky, Eugene R.: Development of Cowling for Long-Nose Air-Cooled Engine in the NACA Full-Scale Wind Tunnel. NACA A.R.R., Oct. 1941.
3. Pinkel, Benjamin, Turner, L. Richard, and Voss, Fred: Design of Nozzles for the Individual Cylinder Exhaust Jet-Propulsion System. NACA A.C.R., April 1941.
4. Bailey, F. J. Jr., Johnston, J. Ford, and Voglowode, T. J.: Flight Investigation of the Performance and Cooling Characteristics of a Long-Nose High-Inlet-Velocity Cowling on the XP-42 Airplane. NACA A.R.R., April 1942.

TABLE Ia.-PRESSURE AND TEMPERATURE DATA

	Flight Run		3-6				3-8				3-9				3-10				3-11
	1	2	1	2	3	4	1	2	3	4	1	2	3	4	1	2	3	4	1
True airspeed, mph	317	334	335	338	334	338	336	335	335	333	333	336	335	336	336	336	336	336	337
Density altitude, ft	1850	1800	1780	1700	1580	1530	1500	1490	1480	1480	1470	1460	1450	1450	1450	1450	1450	1450	1450
Atm press, in. Hg	16.71	16.26	15.74	15.30	14.72	14.16	13.65	13.37	13.08	12.94	12.85	12.66	12.56	12.52	12.52	12.52	12.52	12.52	12.52
Ambient air temp, °F	51	49	49	48	47	45	44	43	42	42	42	41	41	41	41	41	41	41	41
Ground air temp, °F	67	69	69	68	67	65	64	63	62	62	62	61	61	61	61	61	61	61	61
σ, density ratio	1.00	.985	.973	.951	.921	.886	.846	.800	.758	.719	.684	.643	.606	.572	.540	.510	.482	.456	.431
Manifold press, in. Hg	24.0	24.0	24.0	24.0	24.0	24.0	24.0	24.0	24.0	24.0	24.0	24.0	24.0	24.0	24.0	24.0	24.0	24.0	24.0
q, in. Hg	2.54	2.48	2.36	2.24	2.08	1.88	1.64	1.36	1.04	0.78	0.50	0.21	0.00	0.00	0.00	0.00	0.00	0.00	0.00

		Pressure ratio $\frac{p}{p_0}$																			
Engine pressure tube locations	1-R	.39	.40	.42	.41	.42	.41	.40	.40	.38	.39	.39	.39	.39	.39	.39	.39	.39	.39	.39	
	3-R	.39	.40	.42	.41	.42	.41	.40	.40	.38	.39	.39	.39	.39	.39	.39	.39	.39	.39	.39	.39
	4-R	.39	.40	.40	.39	.40	.40	.39	.38	.38	.38	.38	.38	.38	.38	.38	.38	.38	.38	.38	.38
	6-R	.39	.39	.41	.41	.42	.41	.40	.40	.38	.39	.39	.39	.39	.39	.39	.39	.39	.39	.39	.39
	7-R	.39	.40	.42	.41	.42	.41	.40	.40	.38	.39	.39	.39	.39	.39	.39	.39	.39	.39	.39	.39
	9-R	.39	.40	.42	.41	.42	.41	.40	.40	.38	.39	.39	.39	.39	.39	.39	.39	.39	.39	.39	.39
	10-R	.39	.40	.42	.41	.42	.41	.40	.40	.38	.39	.39	.39	.39	.39	.39	.39	.39	.39	.39	.39
	12-R	.39	.40	.42	.41	.42	.41	.40	.40	.38	.39	.39	.39	.39	.39	.39	.39	.39	.39	.39	.39
	14-R	.39	.40	.42	.41	.42	.41	.40	.40	.38	.39	.39	.39	.39	.39	.39	.39	.39	.39	.39	.39
	1-R	.76	.77	.80	.78	.78	.77	.77	.78	.75	.77	.76	.79	.77	.80	.77	.76	.76	.76	.76	.76
	3-TH	.79	.81	.83	.80	.81	.81	.81	.81	.79	.80	.80	.80	.81	.81	.81	.81	.81	.81	.81	.81
	4-TH	.79	.78	.73	.72	.73	.72	.72	.72	.70	.71	.72	.70	.71	.70	.71	.70	.71	.70	.71	.70
	6-TH	.72	.72	.74	.73	.74	.73	.74	.73	.71	.72	.72	.72	.73	.72	.73	.72	.73	.72	.73	.72
	7-TH	.81	.82	.84	.82	.83	.83	.83	.83	.81	.80	.81	.81	.81	.81	.81	.81	.81	.81	.81	.81
9-TH	.82	.84	.85	.83	.84	.84	.84	.83	.81	.83	.83	.82	.83	.83	.83	.83	.83	.83	.83	.83	
10-TH	.74	.75	.78	.75	.77	.76	.73	.73	.74	.73	.75	.74	.73	.74	.73	.74	.73	.74	.73	.73	
12-TH	.75	.74	.75	.73	.78	.74	.73	.73	.72	.73	.72	.72	.73	.72	.73	.72	.73	.72	.73	.72	
14-TH	.89	.71	.73	.71	.72	.71	.71	.71	.69	.71	.70	.69	.70	.70	.70	.70	.70	.70	.70	.70	
1-EH	.84	.84	.89	.86	.87	.87	.86	.84	.84	.86	.86	.86	.86	.86	.86	.86	.86	.86	.86	.86	
3-EH	.78	.78	.81	.79	.79	.78	.78	.74	.77	.77	.78	.77	.77	.77	.77	.77	.77	.77	.77	.77	
4-EH	.88	.84	.90	.89	.90	.89	.89	.90	.82	.89	.88	.88	.84	.88	.85	.85	.85	.85	.85	.85	
5-EH	.81	.83	.85	.84	.83	.83	.83	.83	.80	.82	.82	.81	.81	.81	.81	.81	.81	.81	.81	.81	
7-EH	.84	.86	.84	.86	.87	.87	.87	.86	.86	.85	.85	.85	.85	.85	.85	.85	.85	.85	.85	.85	
9-EH	.86	.87	.89	.83	.86	.85	.85	.84	.84	.84	.84	.84	.84	.84	.84	.84	.84	.84	.84	.84	
10-EH	.86	.88	.90	.87	.88	.87	.87	.87	.86	.86	.87	.86	.86	.87	.86	.87	.86	.87	.86	.87	
12-EH	.86	.87	.87	.88	.88	.87	.87	.86	.83	.85	.85	.84	.84	.84	.84	.84	.84	.84	.84	.84	
14-EH	.83	.84	.83	.84	.83	.84	.83	.84	.82	.83	.83	.82	.83	.82	.82	.82	.82	.82	.82	.82	
1-EB	.84	.83	.87	.83	.85	.84	.84	.84	.83	.83	.83	.84	.84	.83	.83	.83	.83	.83	.83	.83	
3-EB	.84	.70	.72	.70	.71	.70	.70	.70	.69	.69	.70	.69	.70	.69	.70	.69	.70	.69	.70	.69	
4-EB	.81	.83	.85	.83	.83	.83	.83	.82	.80	.82	.82	.82	.83	.82	.83	.82	.83	.82	.83	.82	
6-EB	.81	.81	.83	.81	.83	.81	.81	.82	.80	.81	.81	.81	.81	.81	.81	.81	.81	.81	.81	.81	
7-EB	.81	.81	.83	.81	.83	.81	.81	.82	.80	.81	.81	.81	.81	.81	.81	.81	.81	.81	.81	.81	
9-EB	.82	.85	.86	.83	.84	.83	.84	.83	.82	.83	.83	.83	.83	.83	.83	.83	.83	.83	.83	.83	
10-EB	.77	.77	.80	.78	.80	.79	.79	.78	.77	.77	.77	.77	.77	.77	.77	.77	.77	.77	.77	.77	
12-EB	.78	.80	.82	.80	.80	.80	.80	.79	.78	.79	.79	.79	.79	.79	.79	.79	.79	.79	.79	.79	
14-EB	.78	.80	.82	.80	.80	.80	.80	.79	.78	.79	.79	.79	.79	.79	.79	.79	.79	.79	.79	.79	
1-IN	.82	.82	.84	.82	.84	.82	.82	.81	.81	.81	.82	.81	.81	.81	.81	.81	.81	.81	.81	.81	
6-IN	.87	.88	.90	.84	.90	.88	.84	.89	.86	.85	.88	.88	.88	.84	.88	.84	.88	.84	.88	.84	
10-IN	.89	.91	.93	.91	.93	.91	.92	.90	.89	.90	.90	.91	.92	.91	.91	.91	.91	.91	.91	.91	
1-IB	.77	.78	.81	.79	.78	.78	.78	.76	.77	.78	.77	.78	.77	.78	.77	.78	.77	.78	.77	.78	
6-IB	.83	.86	.88	.86	.87	.86	.85	.84	.83	.85	.85	.85	.85	.85	.85	.85	.85	.85	.85	.85	
10-IB	.82	.82	.83	.83	.83	.82	.82	.83	.82	.82	.82	.83	.82	.81	.82	.81	.82	.81	.82	.81	
3-EH2	.78	.80	.82	.80	.80	.79	.80	.80	.78	.74	.80	.74	.81	.80	.80	.80	.80	.80	.80	.80	
4-EH2	.86	.86	.89	.88	.89	.88	.87	.89	.86	.86	.87	.85	.86	.84	.85	.85	.85	.85	.85	.85	
3-EB2	.84	.86	.87	.86	.87	.86	.86	.85	.84	.84	.85	.84	.84	.84	.84	.84	.84	.84	.84	.84	
4-EB2	.87	.87	.89	.87	.88	.88	.88	.88	.86	.86	.87	.86	.86	.86	.86	.86	.86	.86	.86	.86	

L-383



Method of designating tube locations for typical cylinders

TABLE D.-PRESSURE AND TEMPERATURE DATA

	Flight Run		3-6				3-8				3-9				3-10				3-11				
	2	3	1	2	3	4	1	2	3	4	1	2	3	4	1	2	3	4	1	2			
True air speed, mph	337	336	333	336	339	336	336	337	336	333	333	333	336	337	336	336	337	337	337	337	337		
Density altitude, ft	4360	4360	4360	4360	4350	4350	4350	4350	4350	4350	4350	4350	4350	4350	4350	4350	4350	4350	4350	4350	4350		
Atm. Press., in Hg	16.74	16.74	16.74	16.74	16.74	16.74	16.74	16.74	16.74	16.74	16.74	16.74	16.74	16.74	16.74	16.74	16.74	16.74	16.74	16.74	16.74		
Ambient air temp., °F	81	79	78	75	73	71	71	71	71	71	71	71	71	71	71	71	71	71	71	71	71		
Ground air temp., °F	89	89	89	82	83	82	82	78	71	71	71	71	71	71	71	71	71	71	71	71	71		
σ, density ratio	0.62	0.61	0.61	0.61	0.62	0.62	0.62	0.60	0.60	0.60	0.60	0.60	0.60	0.60	0.60	0.60	0.60	0.60	0.60	0.60	0.60		
POB	2430	2430	2430	2430	2430	2430	2430	2430	2430	2430	2430	2430	2430	2430	2430	2430	2430	2430	2430	2430	2430		
HP	929	985	1021	940	933	912	926	956	923	900	924	927	920	920	927	920	919	922	922	922	922		
Mainline press., in Hg	—	—	—	91.3	90.7	89.0	87.6	91.1	89.3	88.0	86.9	91.1	89.3	88.0	86.9	91.1	89.3	88.0	86.9	91.1	89.3		
% impact press. in H ₂ O	37.9	36.8	33.0	38.3	35.4	32.9	32.2	36.6	32.9	32.7	32.5	36.5	35.9	33.9	33.1	32.5	32.5	32.5	32.5	32.5	32.5		
Pressure ratio, %q																							
		A-TP1 Top survey impact tubes	89	86	88	85	84	83	83	85	84	84	84	85	86	85	85	85	86	85	85	86	
		A-TP2 Top survey impact tubes	92	93	96	94	93	93	93	93	93	93	93	93	93	93	93	93	93	93	93	93	93
		A-TP3 Top survey impact tubes	94	97	98	97	98	93	94	96	96	96	96	96	95	97	95	96	96	96	96	96	96
		A-TP4 Top survey impact tubes	95	97	98	98	96	97	97	97	93	96	95	95	95	96	95	97	97	97	97	97	97
		A-TP5 Top survey impact tubes	90	94	98	91	92	90	90	93	96	92	93	93	90	91	90	90	90	90	90	90	90
		A-TS Static tube	60	60	60	60	60	60	60	67	67	67	67	67	67	67	67	67	67	67	67	67	67
		A-RP1 Right survey impact tubes	84	86	88	84	88	85	84	83	83	83	84	83	83	83	83	84	84	84	84	84	84
		A-RP2 Right survey impact tubes	92	95	96	94	93	93	94	95	95	96	96	96	96	96	96	96	96	96	96	96	96
		A-RP3 Right survey impact tubes	97	98	100	99	100	98	98	99	97	98	99	99	99	99	99	99	99	99	99	99	99
		A-RP4 Right survey impact tubes	97	97	99	97	98	97	97	99	97	97	97	97	95	96	95	96	96	96	96	96	96
A-RP5 Right survey impact tubes	89	90	92	90	90	89	88	90	89	89	88	88	88	89	88	88	88	88	88	88	88		
A-RS Static tube	66	68	68	68	68	67	67	67	68	68	67	67	68	67	68	67	68	67	68	67	67		
		A-LP1 Left survey impact tubes	86	88	89	87	87	86	86	83	86	86	86	86	86	86	86	86	86	86	86	86	
		A-LP2 Left survey impact tubes	99	99	91	96	93	94	94	94	94	94	94	94	94	94	94	94	94	94	94	94	
		A-LP3 Left survey impact tubes	98	99	101	100	100	99	99	99	97	99	99	99	99	99	99	99	99	99	99	99	99
		A-LP4 Left survey impact tubes	97	97	100	98	99	98	98	96	97	97	97	97	98	99	98	98	98	98	98	98	98
		A-LP5 Left survey impact tubes	86	87	89	87	87	88	87	87	85	83	86	87	88	86	87	86	87	86	87	86	87
		A-LS Static tube	72	73	73	73	74	73	73	74	74	73	73	73	73	73	73	73	73	73	73	73	73
		O-FP1 Front survey impact tubes	100	100	100	99	99	98	99	99	97	97	99	99	97	98	97	97	97	97	97	100	
		O-FP2 Front survey impact tubes	100	100	100	100	100	100	100	100	100	100	100	100	100	100	100	100	100	100	100	100	
		O-FP3 Front survey impact tubes	100	100	100	100	100	100	100	100	100	100	100	100	100	100	100	100	100	100	100	100	
		O-FS1 Static tube	91	92	93	93	93	92	92	92	90	90	91	92	90	91	92	91	91	92	91	91	93
		O-FS2 Static tube	92	93	94	93	93	92	92	92	91	91	92	93	91	91	92	92	92	92	92	92	93
		O-FS3 Static tube	96	96	96	96	96	96	96	96	96	96	96	96	96	96	96	96	96	96	96	96	
		O-RP1 Rear survey impact tubes	71	71	73	71	72	71	71	72	69	71	71	70	71	69	70	70	70	70	70	70	72
		O-RP2 Rear survey impact tubes	81	83	85	83	83	83	82	83	86	83	82	81	81	81	81	81	81	81	81	81	83
		O-RP3 Rear survey impact tubes	89	81	83	80	81	80	80	79	78	79	80	78	79	79	79	79	79	79	79	79	80
		O-SP Static tube	59	60	62	60	60	60	59	59	57	58	58	58	58	58	58	58	58	58	58	58	58
		C-P1 Impact tubes	108	108	109	103	104	103	103	103	102	101	101	101	101	101	101	101	101	101	101	101	
		C-P2 Impact tubes	108	109	106	103	104	103	104	103	103	104	103	103	103	103	103	103	103	103	103	103	103
		C-P3 Impact tubes	109	106	107	105	106	104	105	105	109	104	105	105	105	105	105	105	105	105	105	105	105
		C-P4 Impact tubes	105	107	109	109	107	106	106	109	103	103	103	103	103	103	103	103	103	103	103	103	103
		C-P5 Impact tubes	106	107	109	107	107	106	106	107	105	106	106	106	106	106	106	106	106	106	106	106	106
		C-S1 Static tubes	86	86	88	86	87	87	86	86	83	86	86	85	83	84	84	84	84	84	84	84	84
		C-S2 Static tubes	89	84	86	89	85	84	84	84	84	84	84	84	84	84	84	84	84	84	84	84	84
		C-S3 Static tubes	83	89	87	89	89	84	89	89	82	83	84	84	84	84	84	84	84	84	84	84	84
		C-S4 Static tubes	84	84	87	84	83	84	84	83	83	84	84	84	84	84	84	84	84	84	84	84	84
		C-S5 Static tubes	86	85	87	89	85	84	85	85	84	84	84	84	84	84	84	84	84	84	84	84	84

L-383

TABLE Ic.—PRESSURE AND TEMPERATURE DATA

Test - flight run	3-6				3-8				3-9				3-10				3-11
	2	3	4	1	2	3	4	1	2	3	4	1	2	3	4		
True airspeed, mph	337	334	333	331	334	336	336	335	337	335	333	336	336	336	337		
Density altitude, ft	16350	16200	16200	16000	15700	15500	15500	15500	15400	15300	15300	15200	15000	14800	14800		
Atm press, in. Hg	16.71	16.25	16.74	17.30	16.71	16.16	15.65	15.37	16.21	15.96	15.65	15.26	14.85	14.52	14.21		
Ambient air temp, °F	21	19	16	15	15	9	5	12	12	10	8	19	18	18	5		
Ground air temp, °F	67	67	67	62	62	62	62	74	72	71	73	60	61	62	63		
σ, density ratio	0.61	0.61	0.73	0.81	0.82	0.91	0.92	0.93	0.94	0.94	0.94	0.85	0.87	0.87	0.73		
RPM	2680	2687	2626	2617	2630	2630	2640	2630	2630	2630	2630	2704	2704	2700	2700		
BHP	924	885	112	924	933	972	976	970	933	888	872	947	923	884	851		
Manifold press, in. Hg	—	—	—	41.2	39.7	38.0	37.4	41.1	39.5	38.0	36.4	41.1	39.7	38.7	38.1		
Ice impact press, in. Hg	354	348	338	373	354	349	341	346	350	337	321	367	354	349	321		

Cylinder—point of measurement	Temperature °F															
	1				2				3				4			
gasket thermocouple at rear spark plug	thermocouple broken															
1	370	372	403	360	368	390	433	370	370	379	362	364	393	398	394	
2	405	390	403	399	—	397	410	392	383	392	380	370	395	400	400	
3	372	372	394	366	368	390	397	376	376	379	364	364	393	391	391	
4	thermocouple broken															
5	367	367	392	362	365	369	376	360	363	367	366	362	366	364	370	
6	430	428	430	421	426	424	420	417	419	419	410	422	429	429	423	
7	384	381	390	361	374	387	387	365	372	376	373	375	379	382	366	
8	415	414	426	406	408	408	414	397	403	403	395	407	407	407	404	
9	401	403	432	414	415	421	420	410	413	415	410	418	412	412	411	
10	428	430	437	424	428	428	433	415	418	417	410	422	413	409	420	
11	403	403	414	399	399	406	410	396	394	397	400	400	400	400	400	
12	404	408	425	414	421	424	423	412	415	417	423	422	420	421	421	
13	421	424	432	414	412	419	420	405	405	410	414	414	412	423	420	
14	thermocouple broken															
1	311	307	311	302	302	302	311	297	297	300	291	303	307	309	309	
2	300	300	302	293	293	295	300	286	286	282	294	296	296	298	294	
3	302	302	304	299	299	295	300	286	286	283	293	292	294	298	294	
4	288	288	290	282	284	286	282	275	275	279	287	287	287	287	287	
5	304	304	304	297	297	300	304	283	284	293	303	303	303	303	303	
6	292	290	293	286	286	287	291	274	280	282	289	289	289	289	282	
7	295	293	297	290	287	293	295	286	286	288	287	290	290	290	284	
8	306	311	311	302	302	302	307	298	297	302	301	303	303	303	305	
9	320	320	326	310	316	318	320	309	309	311	310	316	314	314	317	
10	293	297	297	286	286	288	293	282	282	288	289	290	294	290	284	
11	311	320	324	309	311	313	318	304	304	306	310	312	314	314	314	
12	300	302	304	290	292	297	304	293	289	293	296	299	303	303	303	
13	311	311	311	304	304	306	313	297	297	300	303	307	308	308	308	
14	283	287	288	275	277	277	277	274	270	270	277	277	278	278	278	
10 — intake port	no temperature record															
Mixture at blower rim	83	86	88	88	89	88	88	87	87	87	87	87	87	87	86	
Fuel on suction side of pump	71	81	84	81	82	81	81	77	75	77	71	71	71	75	78	
" " pressure	84	90	90	83	85	85	84	81	77	81	78	82	78	84	78	
" at outlet of flow meter	80	82	83	80	82	82	80	84	84	84	82	83	82	87	80	
" in carburetor float chamber	74	80	80	80	82	82	86	79	75	75	78	78	82	82	76	
1 — front spark plug elbow	44	46	46	43	49	49	49	60	60	60	44	44	44	44	40	
1 — rear " " "	60	64	62	61	77	77	72	72	68	64	70	70	74	71	71	
7 — front " " "	46	44	48	39	39	34	39	46	49	53	49	49	46	49	40	
7 — rear " " "	33	64	64	32	32	48	34	46	43	36	53	49	40	40	40	
11 — front " " "	58	46	49	46	42	43	39	43	39	36	49	46	40	37	36	
11 — rear " " "	81	81	81	77	77	77	72	66	68	69	70	72	74	71	71	
Recorded free air	39	39	34	33	32	27	33	36	30	35	37	31	28	27	23	
Pkts. absorbs free air	37	37	34	36	33	31	39	35	32	24	33	29	25	23	17	
Air in carburetor scoop	44	46	48	40	39	34	36	39	32	30	46	42	37	33	31	
" at top annular scoop	42	46	48	46	39	34	36	39	36	32	46	40	37	33	31	
" in front of cylinder 1.	34	34	38	32	38	40	43	40	39	36	49	47	46	40	39	
" behind cylinder 1.	109	102	100	113	109	116	107	121	—	—	—	—	—	—	—	
" at exit from oil cooler	81	81	81	77	72	70	72	68	61	57	74	71	69	62	61	
Oil in line	138	138	138	133	133	133	133	121	123	124	134	134	132	132	132	
" out	24	24	24	208	208	207	207	203	201	201	206	206	208	204	200	
Accessory compartment	154	159	154	154	120	118	132	109	109	62	119	119	116	116	110	
Right magneto	thermocouple broken															
Left " " "	100	108	108	106	106	106	102	97	93	97	107	103	102	100	100	
Pilot's cockpit (recorded)	70	77	97	90	90	90	82	20	82	84	91	87	80	87	76	
" (observed)	—	—	—	90	70	70	69	62	60	62	64	—	—	—	—	
Recording instrument compartment	62	93	93	116	84	36	84	61	81	77	87	87	85	83	76	

4-383

TABLE II
AVERAGE COOLING AIR PRESSURES AT SEVERAL LOCATIONS ON FRONT AND REAR CYLINDERS

Locations	Flight				3-6				3-8				3-9				3-10				3-11		
	2	3	4	5	1	2	3	4	1	2	3	4	1	2	3	4	1	2	3	4	1	2	
Top of heads	0.72	0.73	0.73	0.73	0.73	0.73	0.73	0.73	0.73	0.73	0.73	0.73	0.73	0.73	0.73	0.73	0.73	0.73	0.73	0.73	0.73	0.73	0.73
Exhaust side of heads	0.80	0.81	0.83	0.83	0.81	0.81	0.82	0.80	0.80	0.80	0.80	0.80	0.80	0.80	0.80	0.80	0.80	0.80	0.80	0.80	0.80	0.80	0.80
Exhaust side of barrels	0.84	0.84	0.87	0.87	0.84	0.84	0.85	0.84	0.84	0.84	0.84	0.84	0.84	0.84	0.84	0.84	0.84	0.84	0.84	0.84	0.84	0.84	0.84
Intake side of heads	0.78	0.80	0.82	0.82	0.80	0.80	0.81	0.80	0.80	0.80	0.80	0.80	0.80	0.80	0.80	0.80	0.80	0.80	0.80	0.80	0.80	0.80	0.80
Intake side of barrels	0.79	0.80	0.82	0.82	0.80	0.80	0.81	0.80	0.80	0.80	0.80	0.80	0.80	0.80	0.80	0.80	0.80	0.80	0.80	0.80	0.80	0.80	0.80
Topmost fin on exhaust side of heads	0.88	0.90	0.92	0.92	0.90	0.90	0.92	0.90	0.90	0.90	0.90	0.90	0.90	0.90	0.90	0.90	0.90	0.90	0.90	0.90	0.90	0.90	0.90
Lowest fin on exhaust side of barrels	0.82	0.82	0.84	0.84	0.82	0.82	0.84	0.82	0.82	0.82	0.82	0.82	0.82	0.82	0.82	0.82	0.82	0.82	0.82	0.82	0.82	0.82	0.82
Topmost fin on exhaust side of heads	0.84	0.84	0.87	0.87	0.84	0.84	0.85	0.84	0.84	0.84	0.84	0.84	0.84	0.84	0.84	0.84	0.84	0.84	0.84	0.84	0.84	0.84	0.84
Lowest fin on exhaust side of barrels	0.77	0.78	0.81	0.81	0.79	0.78	0.78	0.78	0.78	0.78	0.78	0.78	0.78	0.78	0.78	0.78	0.78	0.78	0.78	0.78	0.78	0.78	0.78
Topmost fin on exhaust side of heads	0.86	0.86	0.89	0.89	0.88	0.89	0.88	0.88	0.88	0.88	0.88	0.88	0.88	0.88	0.88	0.88	0.88	0.88	0.88	0.88	0.88	0.88	0.88
Lowest fin on exhaust side of barrels	0.78	0.80	0.82	0.82	0.80	0.80	0.80	0.79	0.80	0.80	0.80	0.80	0.80	0.80	0.80	0.80	0.80	0.80	0.80	0.80	0.80	0.80	0.80
Topmost fin on exhaust side of heads	0.67	0.69	0.70	0.68	0.68	0.69	0.68	0.68	0.68	0.68	0.68	0.68	0.68	0.68	0.68	0.68	0.68	0.68	0.68	0.68	0.68	0.68	0.68
Lowest fin on exhaust side of barrels	0.64	0.66	0.67	0.66	0.66	0.67	0.66	0.66	0.66	0.66	0.66	0.66	0.66	0.66	0.66	0.66	0.66	0.66	0.66	0.66	0.66	0.66	0.66

¹Based on cylinders 6 and 10.

²Based on cylinder 1.

³Based on cylinder 4.

⁴Based on cylinder 3.

L-383

1-3-37
NACA

25
Fig. 1.2.3



Figure 1.- Front view of XP-42 airplane with short-nose high-inlet-velocity cowling.

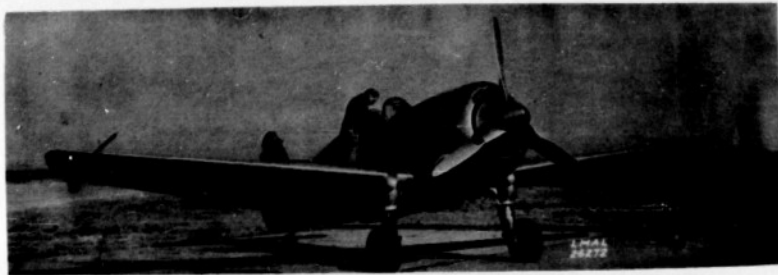


Figure 2.- Three-quarter front view of the XP-42 airplane with short-nose high-inlet-velocity cowling.



Figure 3.- Side view of the XP-42 airplane with short-nose high-inlet-velocity cowling.

NACA

Fig. 4

26

L-383

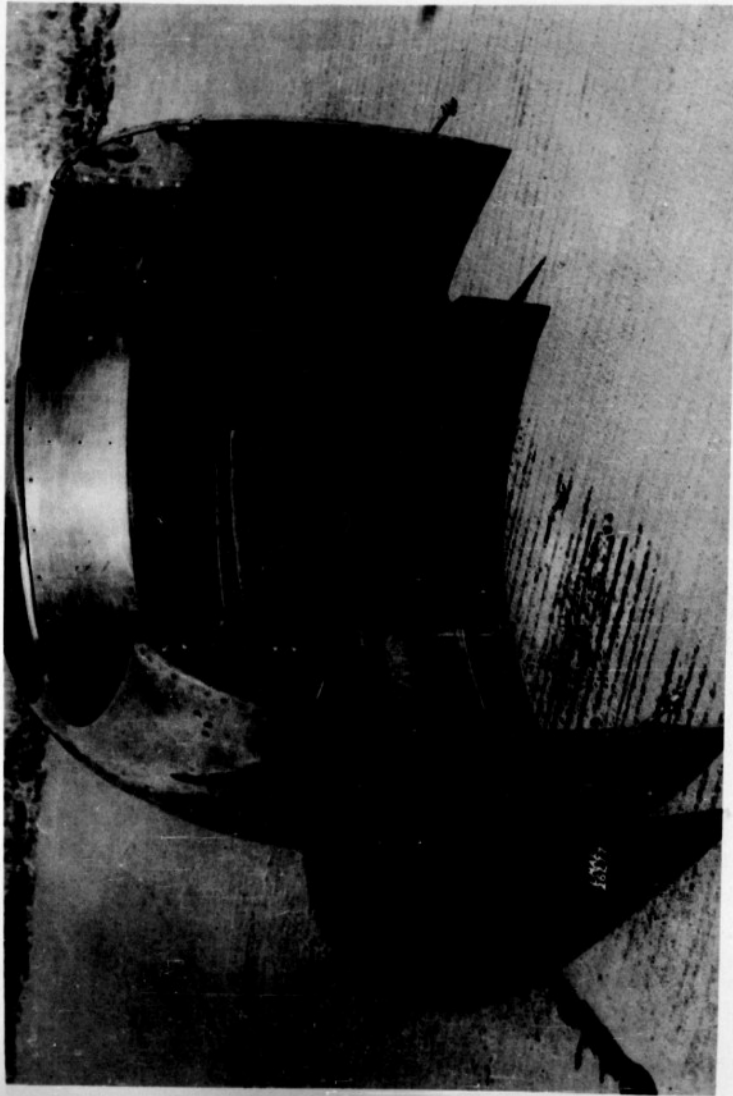


Figure 4.- Upper part of short-nose high-inlet-velocity cowling.

4-383
NACA

27
Fig. 5

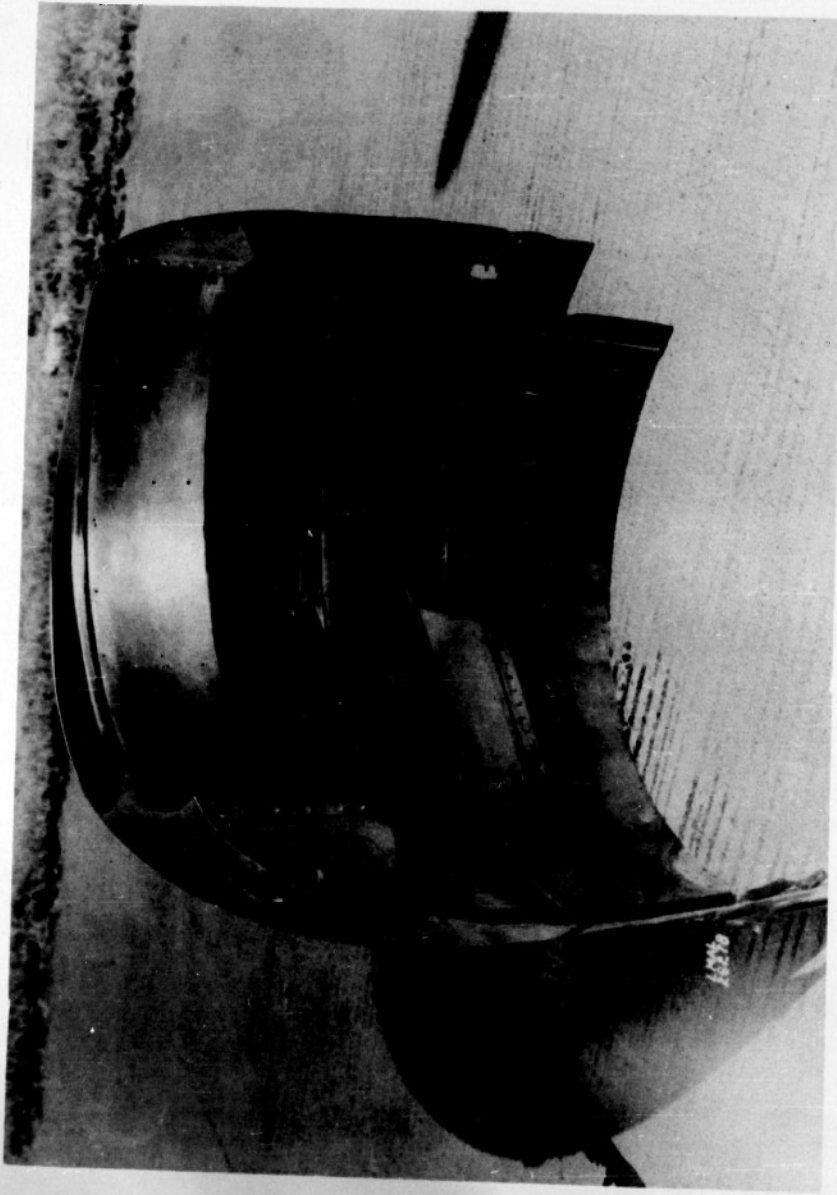


Figure 5.- Lower part of short-nose high-inlet-velocity cowl.

5-25-7

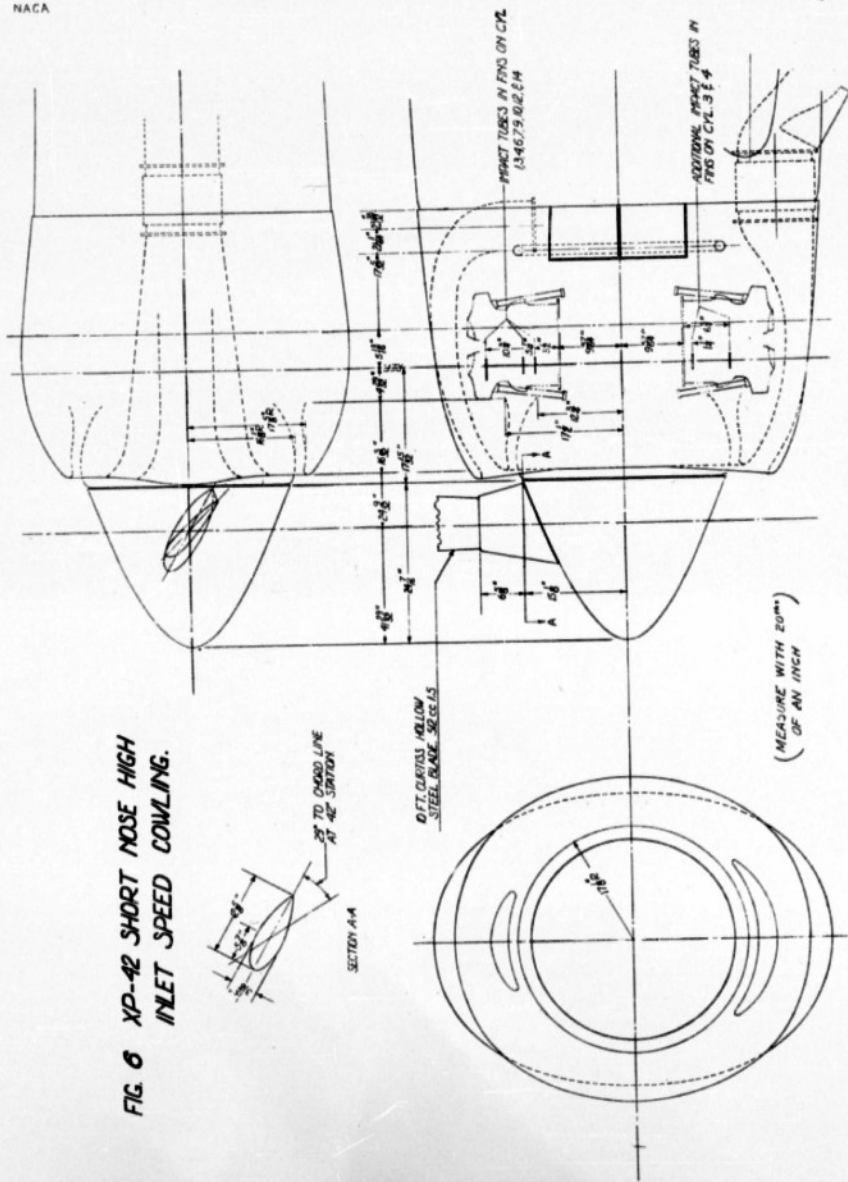


FIG. 6 XP-42 SHORT NOSE HIGH INLET SPEED COWLING.

4-383

NACA

Fig. 7

29



Figure 7.- Airspeed boom on right wing.

2-303

NACA

Figs. 8,9 ³⁰

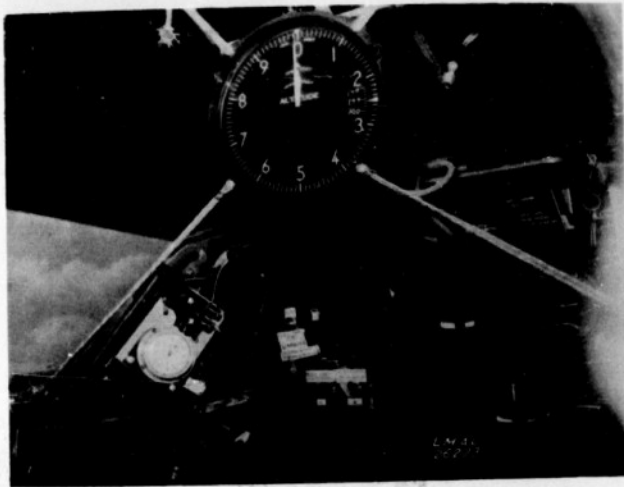


Figure 8.- Sensitive altimeter used in calibrating
airspeed head.

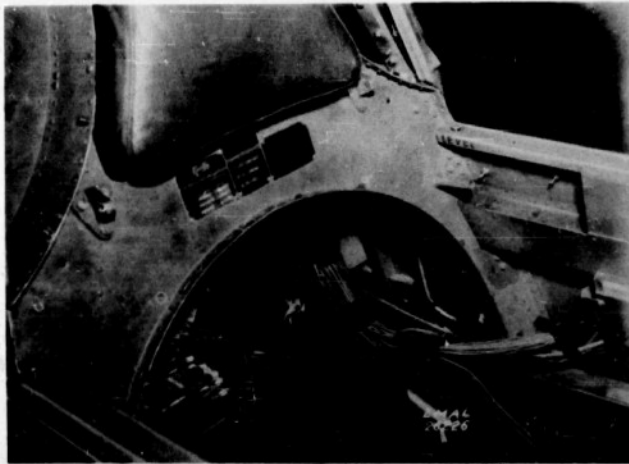


Figure 9.- Thermocouple leads to cold-junction box.

2-383
NACA

3'
Figs. 10,11



Figure 10.- Free-air thermocouple and vapor-pressure thermometer.

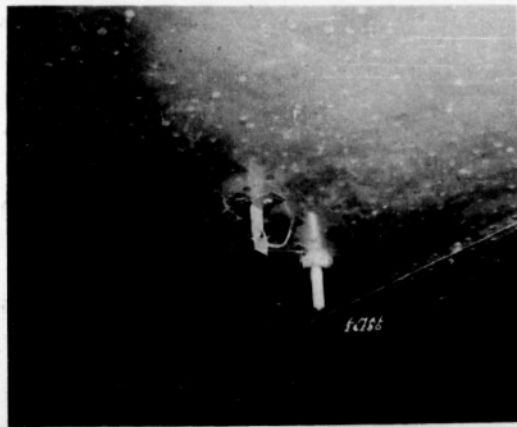


Figure 11.- Free-air thermocouple and resistance-bulb thermometer.

NACA

Figs. 12,13

4-383

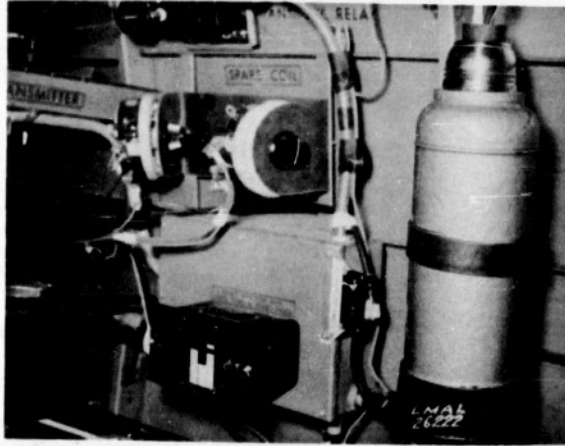


Figure 12.- Thermos bottle used as hot junction.



Figure 13.- Pressure-switch installation over manometer.

6-3-53
NACA

Figs. 14,17,19

33

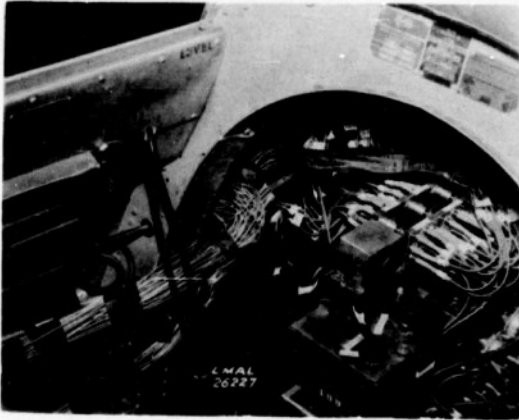


Figure 14.-
Manometer
and
pressure-
switch
installation.

Figure 17.-
Rear part
of
carburetor
duct,
showing
pressure
rakes.

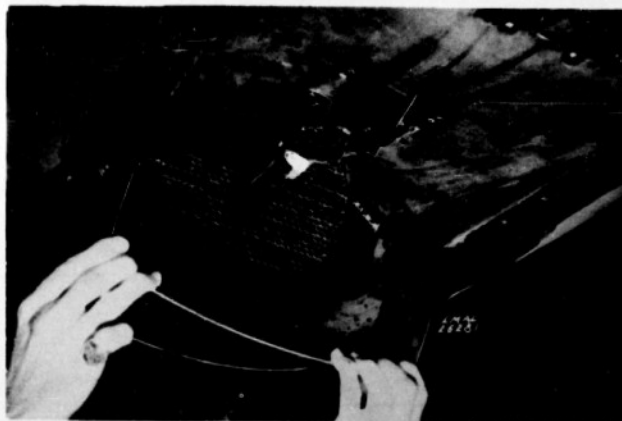
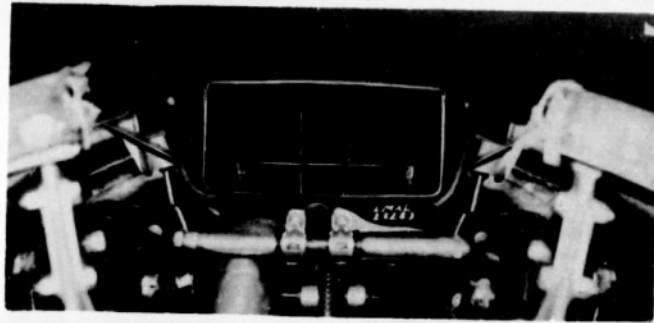


Figure 19.-
Rear
of
oil
cooler.

4-383

NACA

Fig. 15 34

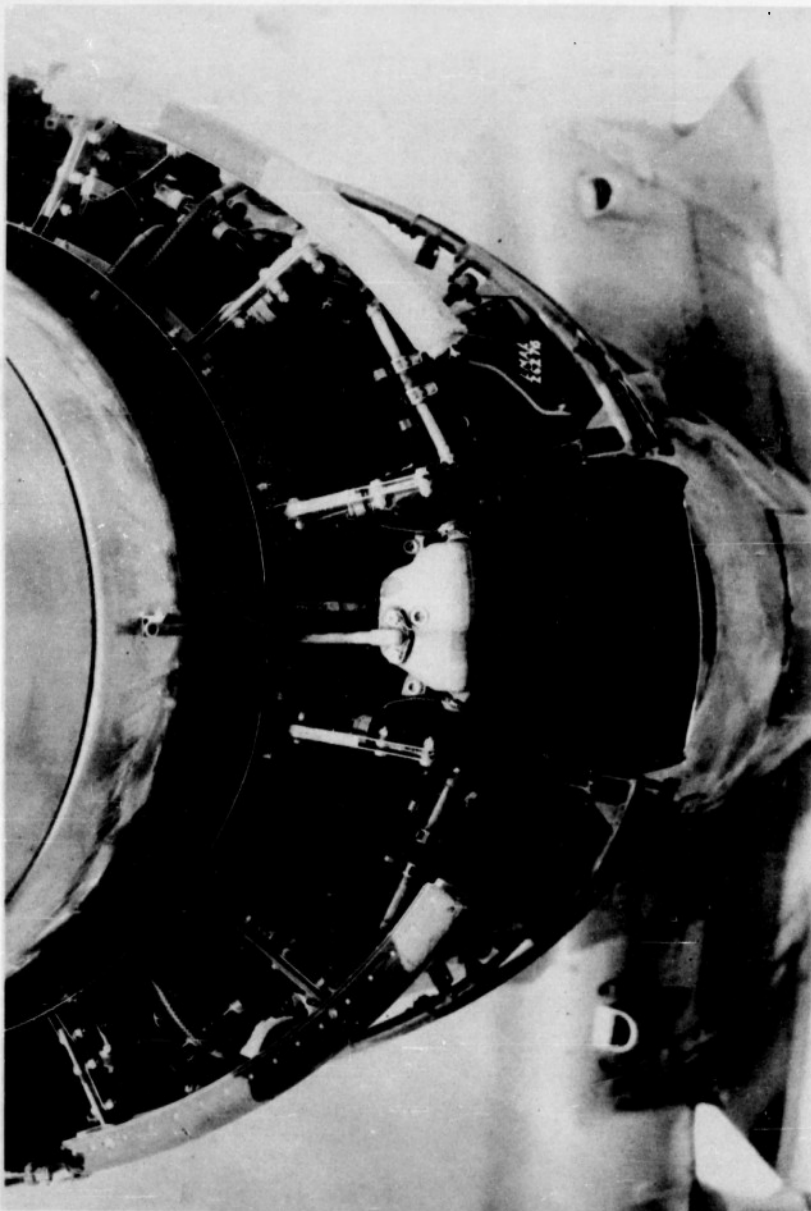


Figure 15.- Front of engine with cowling removed, showing right and left pressure rakes in annulus.

12-383

NACA

Fig. 16

35

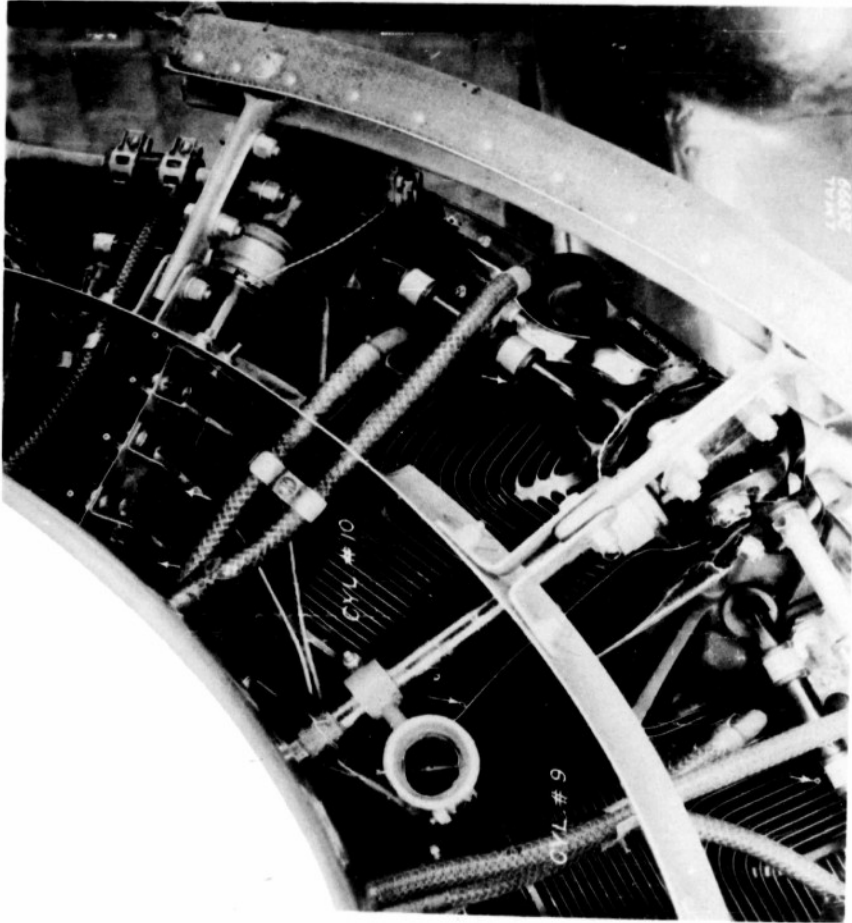


Figure 16.-
Pressure
tubes in
baffles of
cylinder
10.

NACA

Fig. 18 36

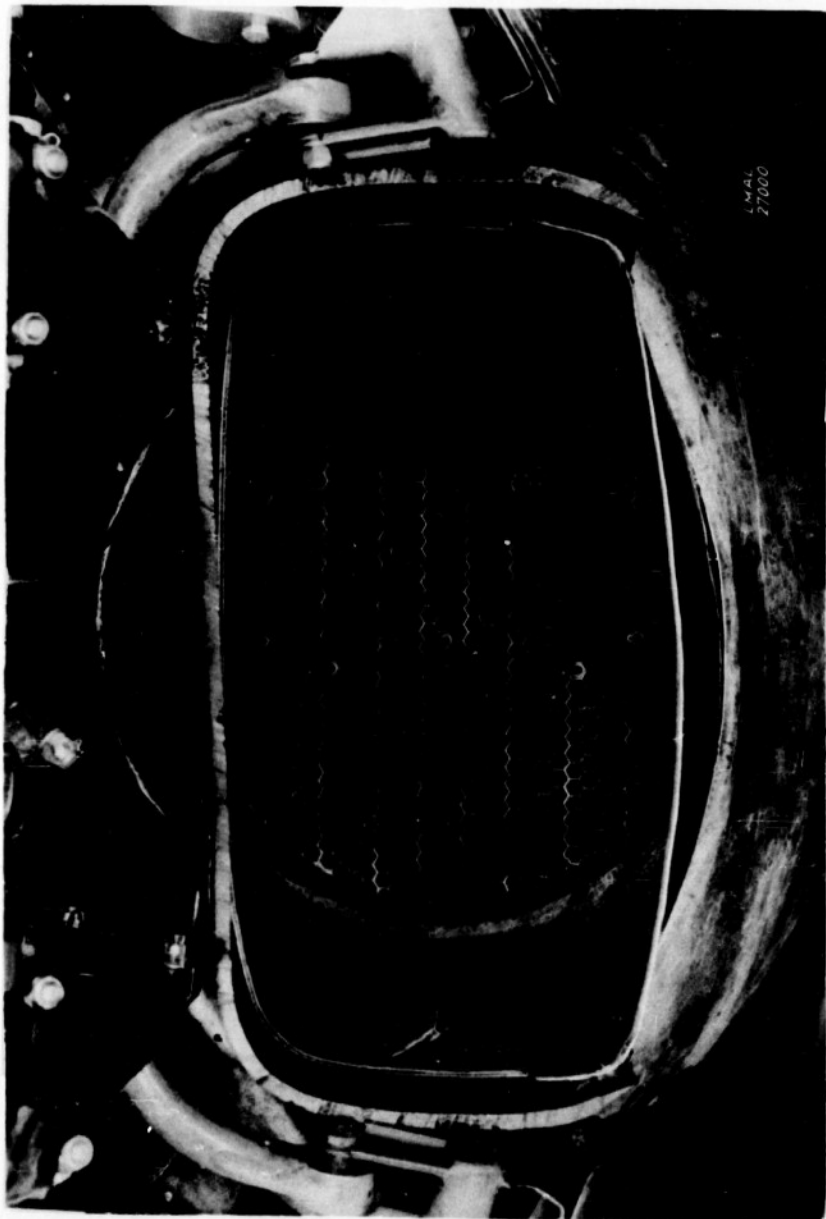
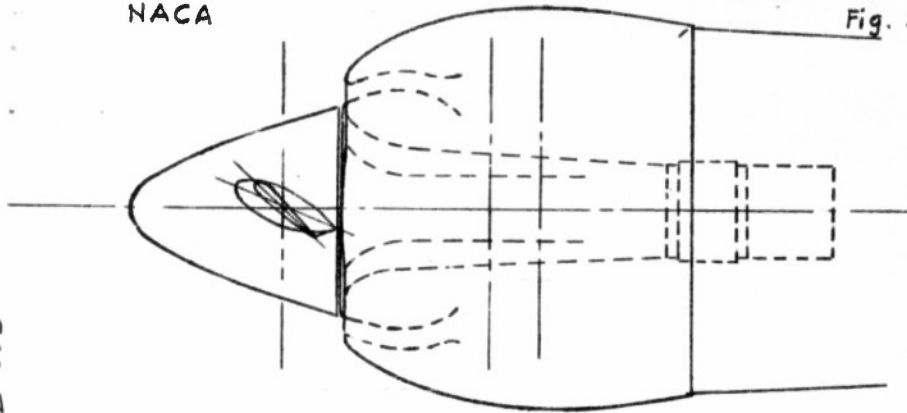


Figure 18.- Face of oil cooler, showing pressure tubes.

NACA

37

Fig. 20



TOP VIEW

1 Static & 5 impact tubes
at 0, 120°, & 240° from top
annular entrance

5 impact & 3 static tubes
along vertical & of
carb. inlet duct.

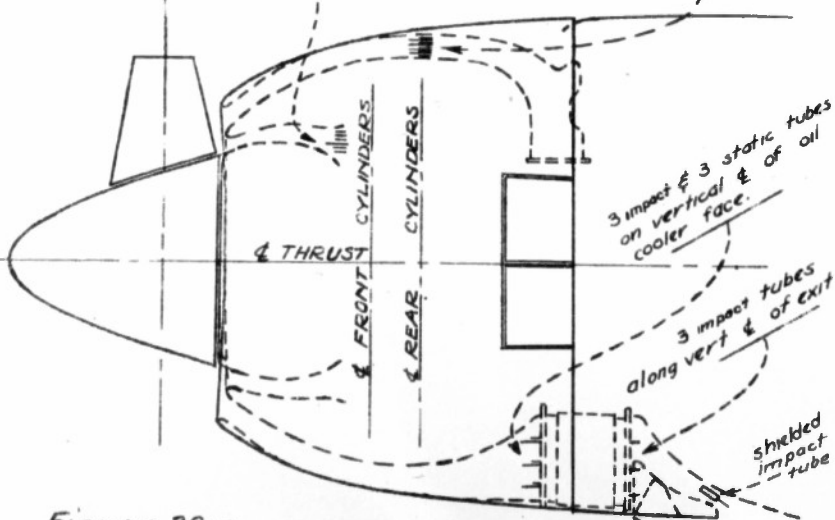


Figure 20.-

XP-42 SHORT-NOSE HIGH-INLET VELOCITY COWLING,

4-383

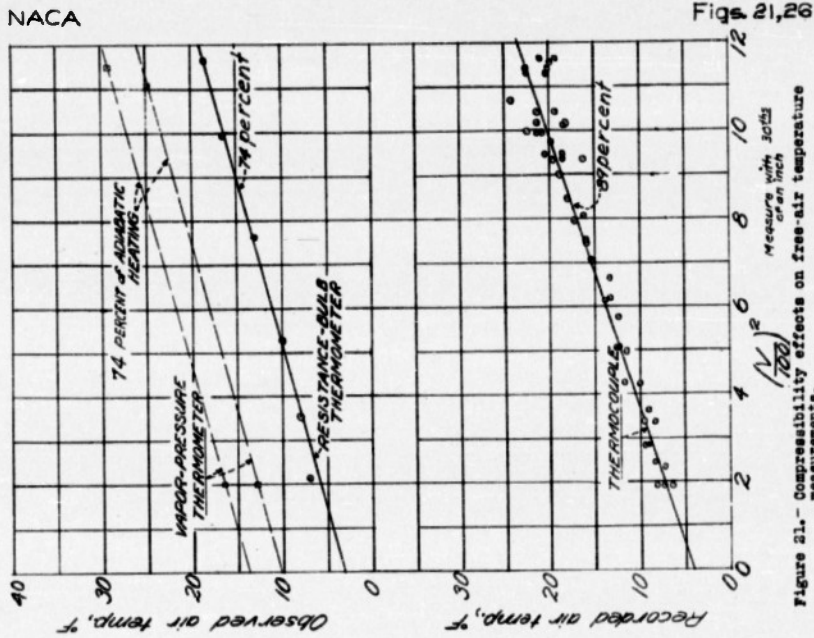


Figure 21.- Compressibility effects on free-air temperature measurements.

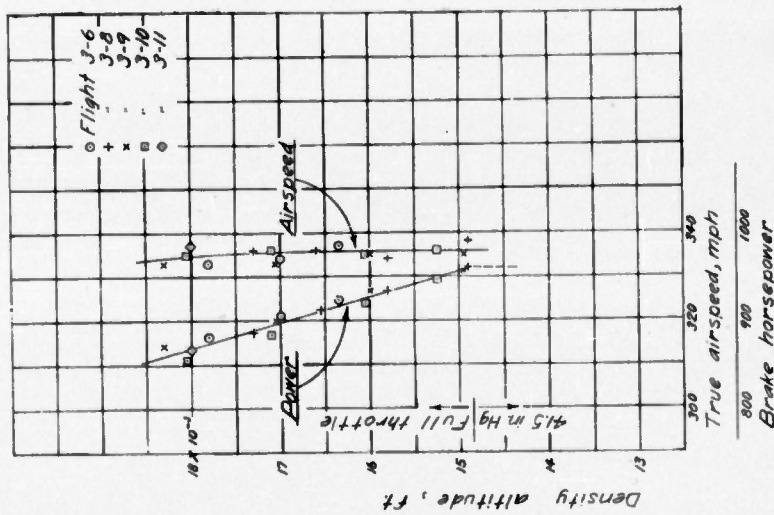


Figure 26.- Variation of airspeed and power with density altitude.

L-383

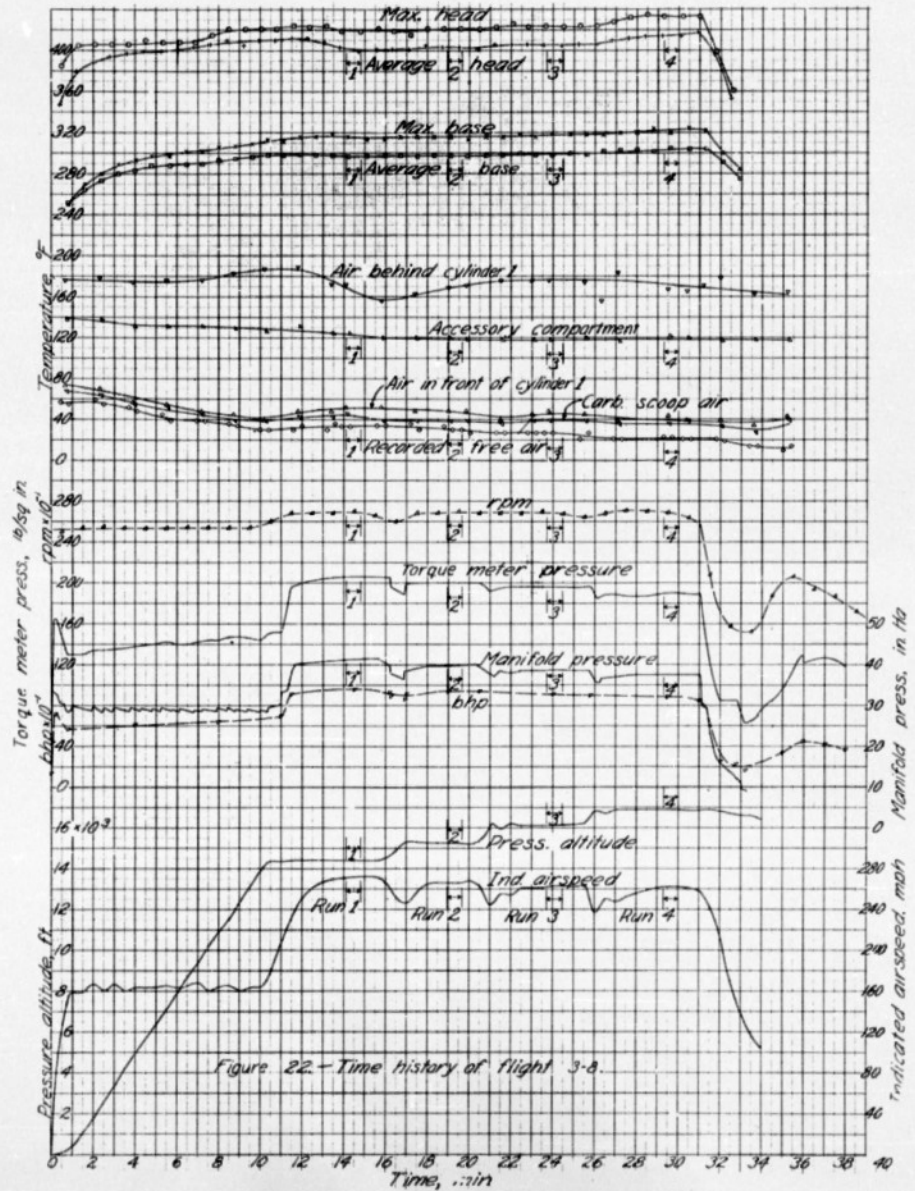


Figure 22 - Time history of flight 3-8.

NACA

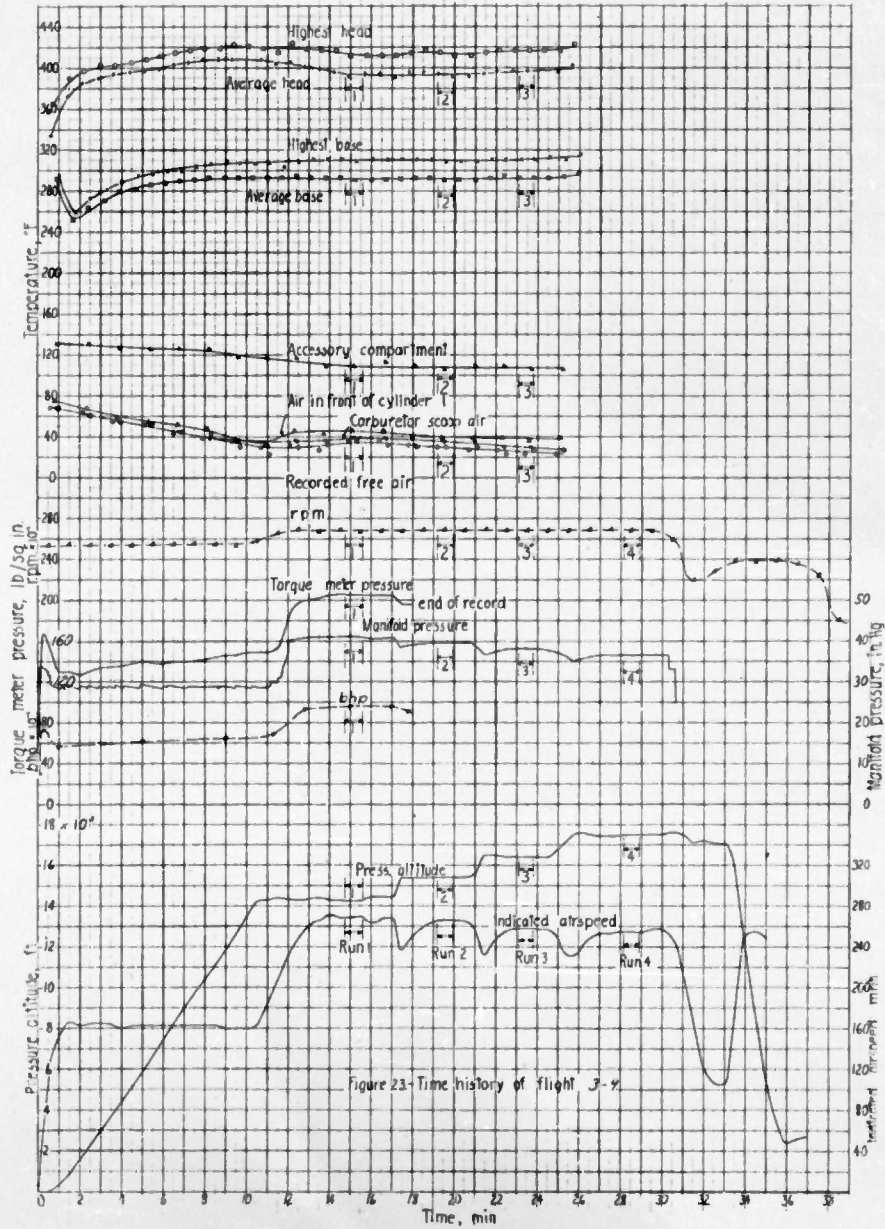


Figure 23 - Time history of flight 3-4

NACA

Fig 24

2-3-33

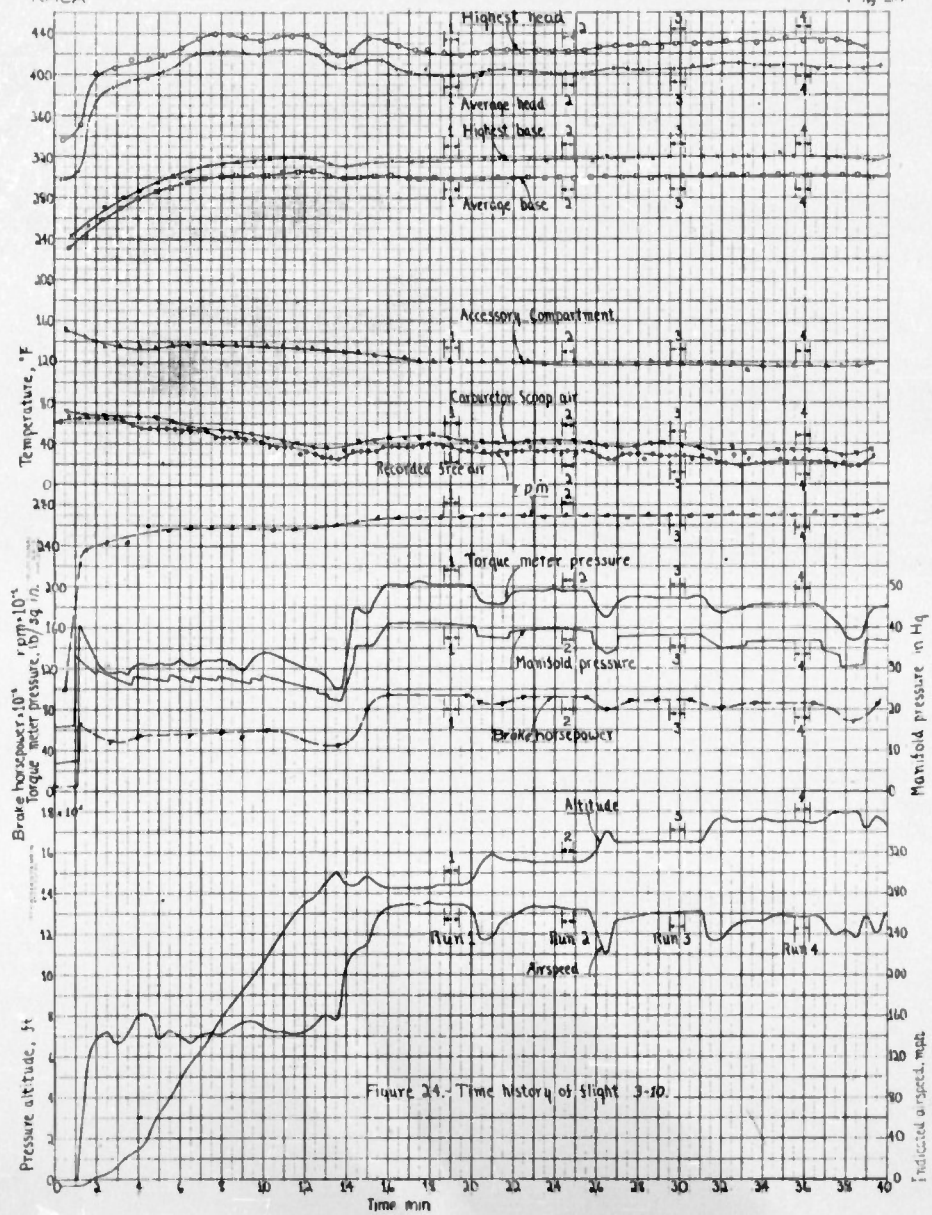


Figure 24 - Time history of flight 3-20.

L-383

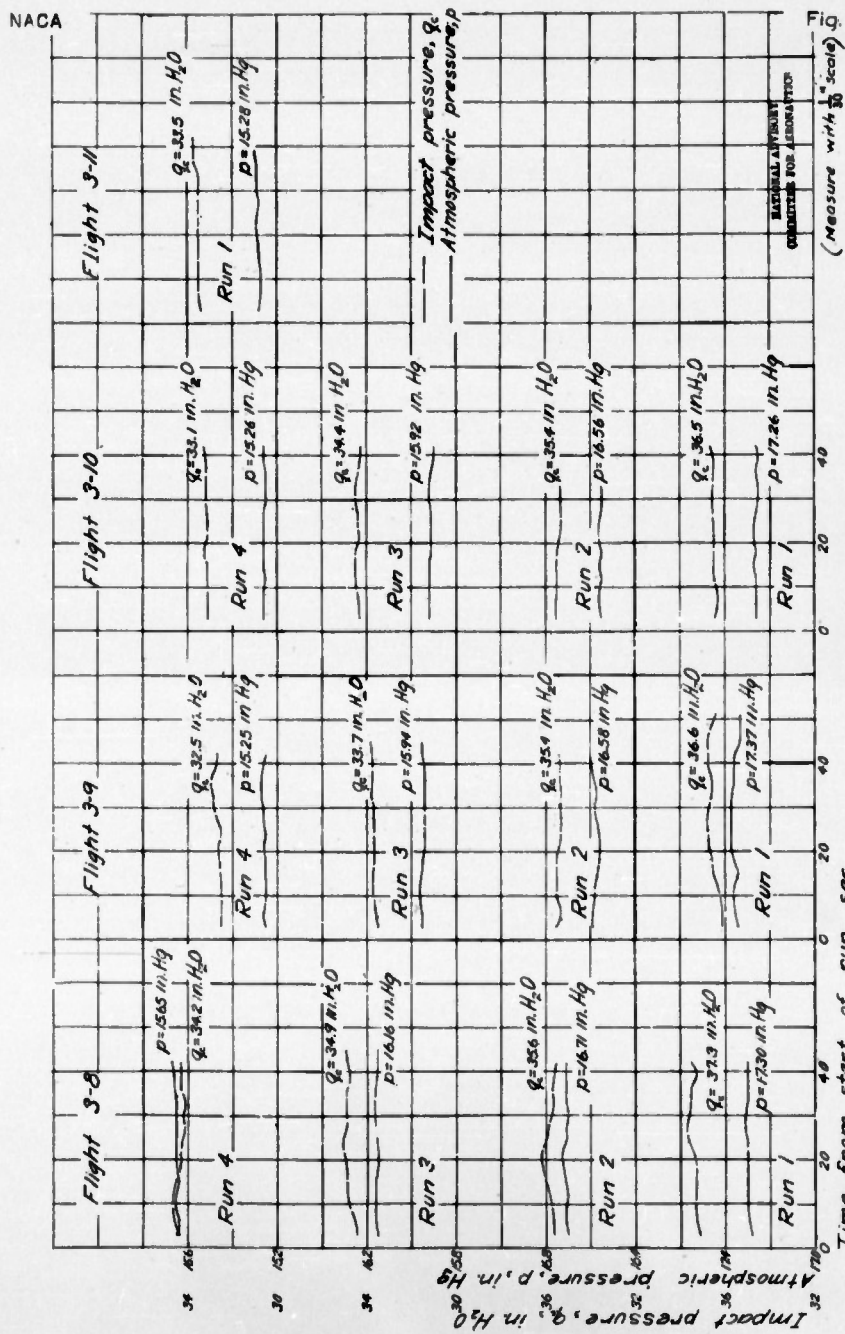
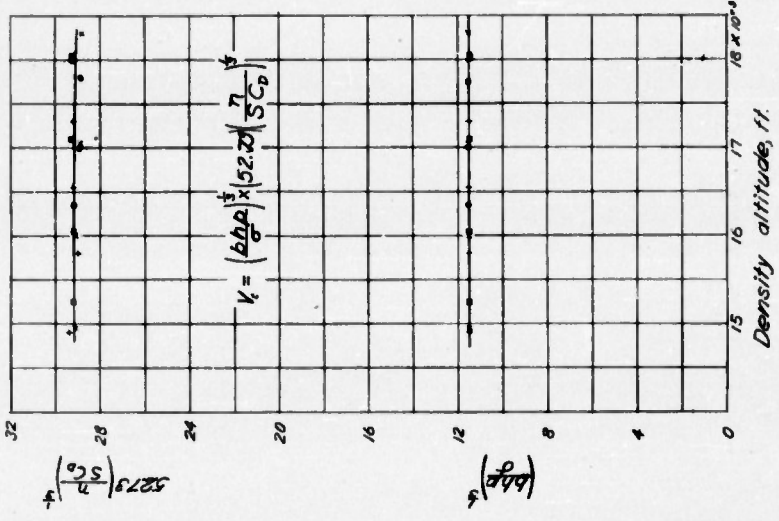


Figure 25. - Time histories of atmospheric and impact pressures during high-speed runs.

NACA

Figs 27,28

4-283



(Measure with 30ths of an inch)
Figure 27.- Analysis of high-speed performance.

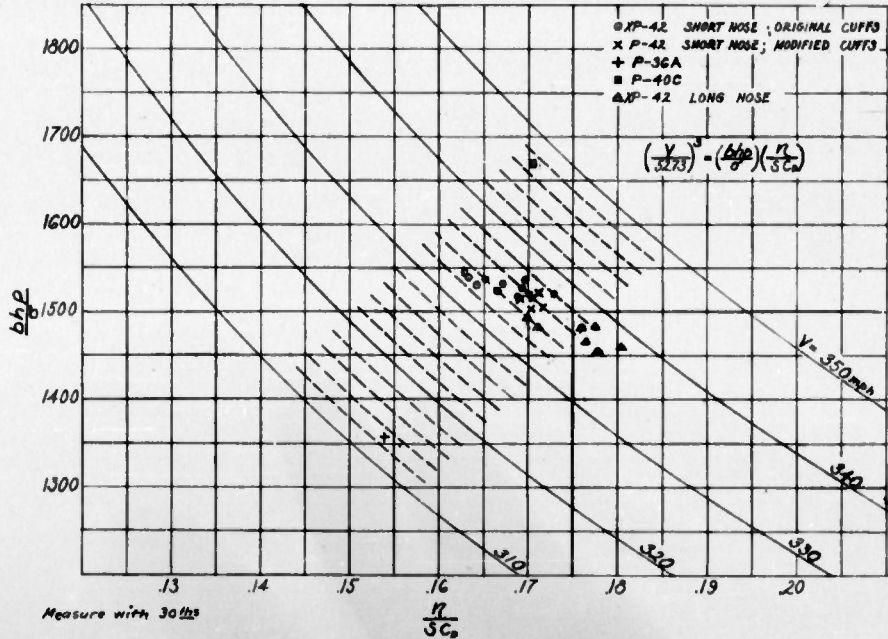


Figure 28.- Comparison of high-speed performance on several airplanes.

L 385-7

NACA

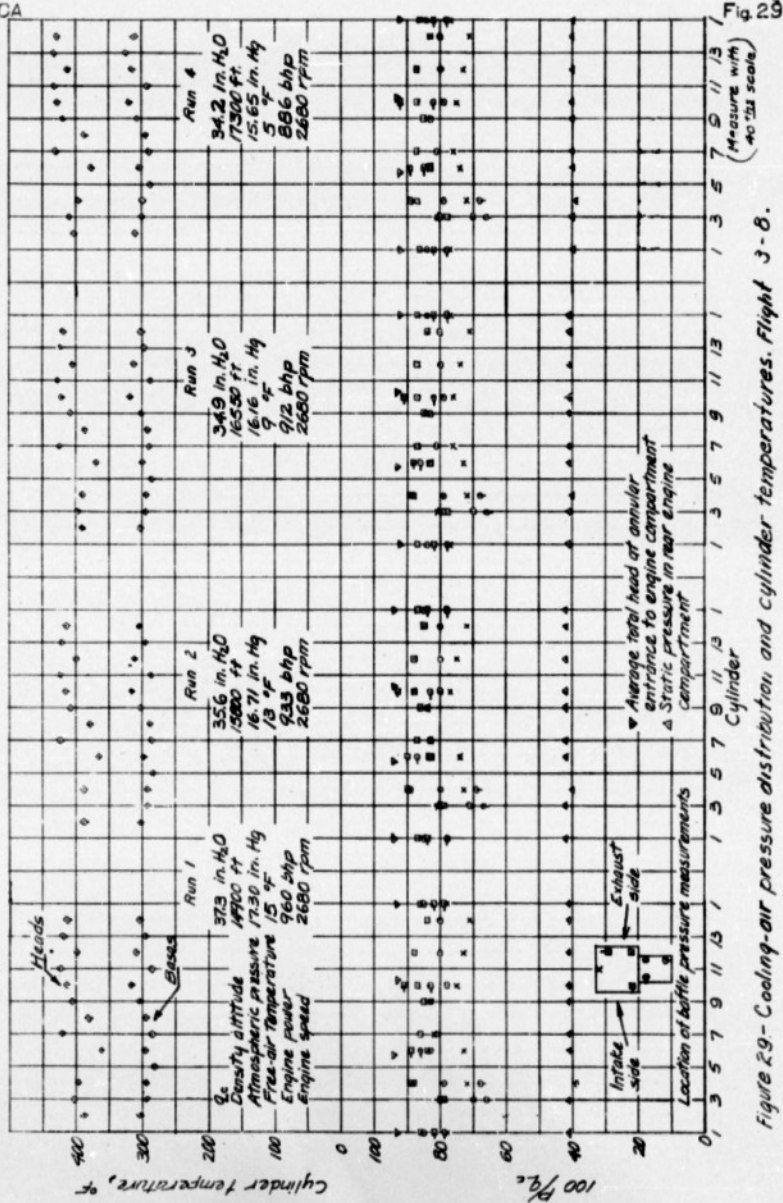


Figure 29.-Cooling-air pressure distribution and cylinder temperatures. Flight 3-8.

4-383

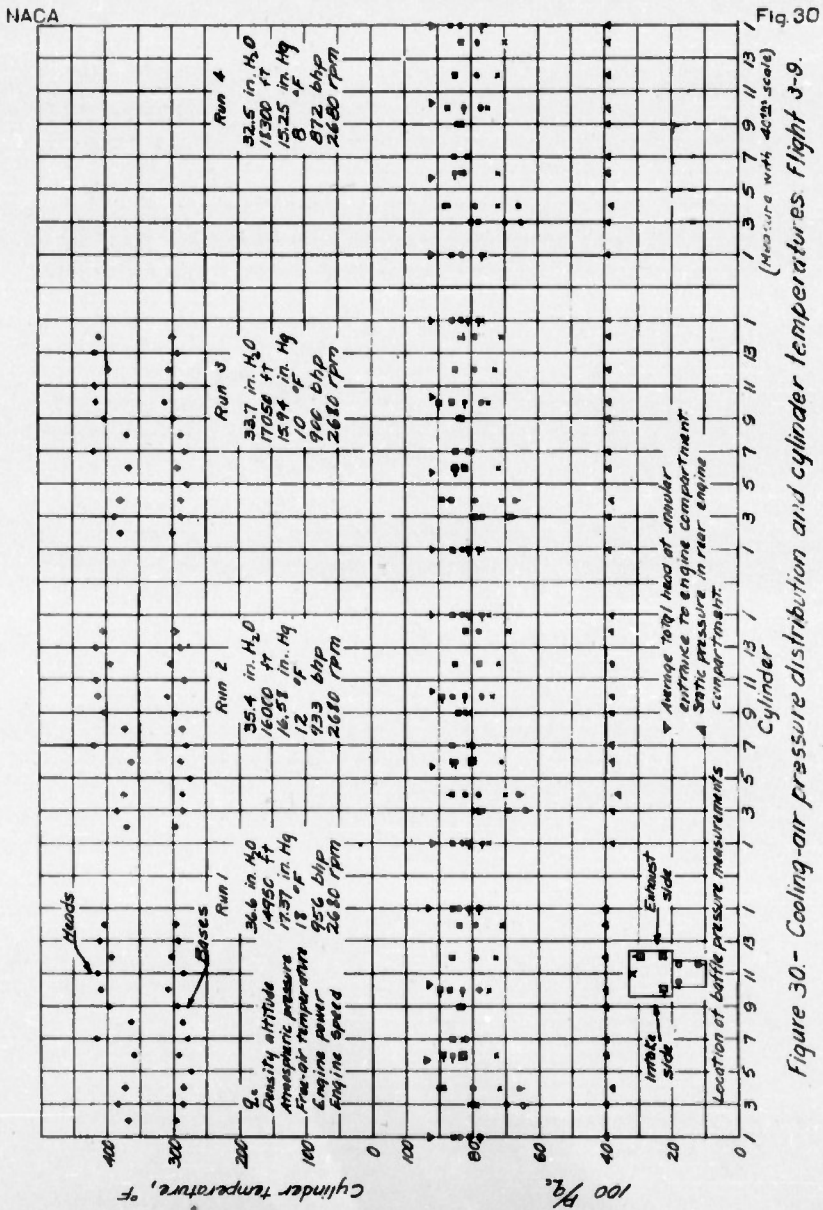


Figure 30.- Cooling-air pressure distribution and cylinder temperatures Flight 3-9.

NACA

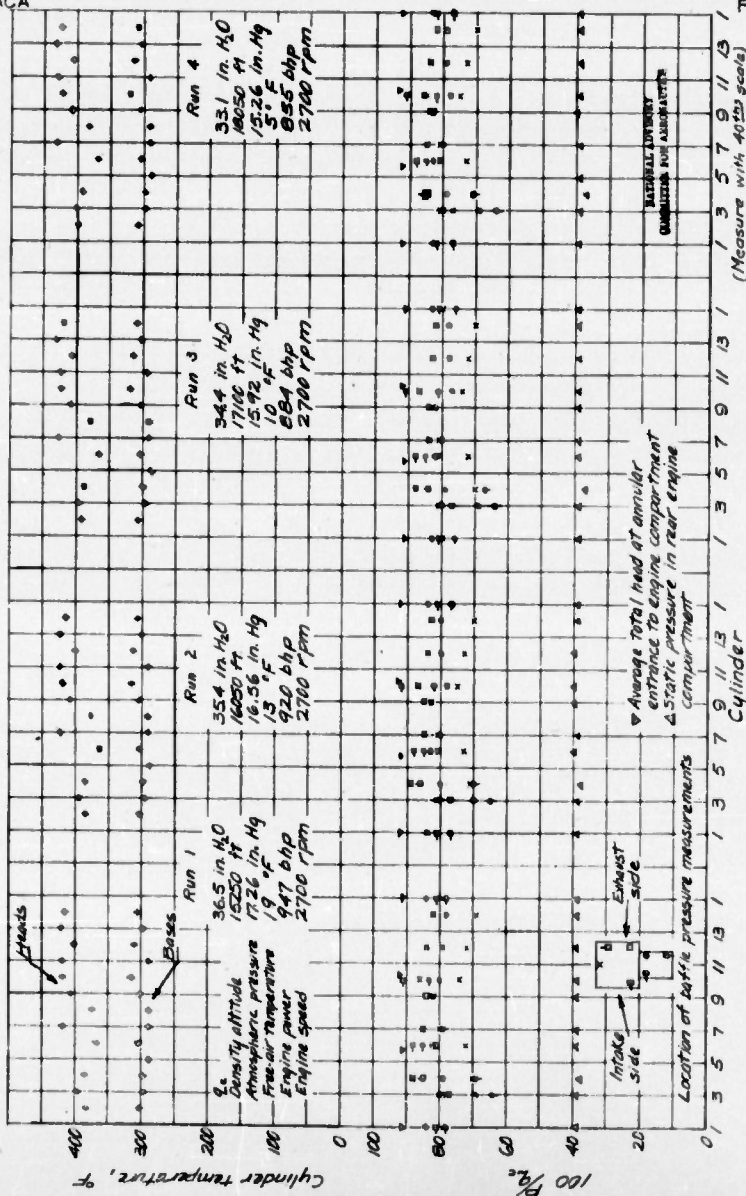
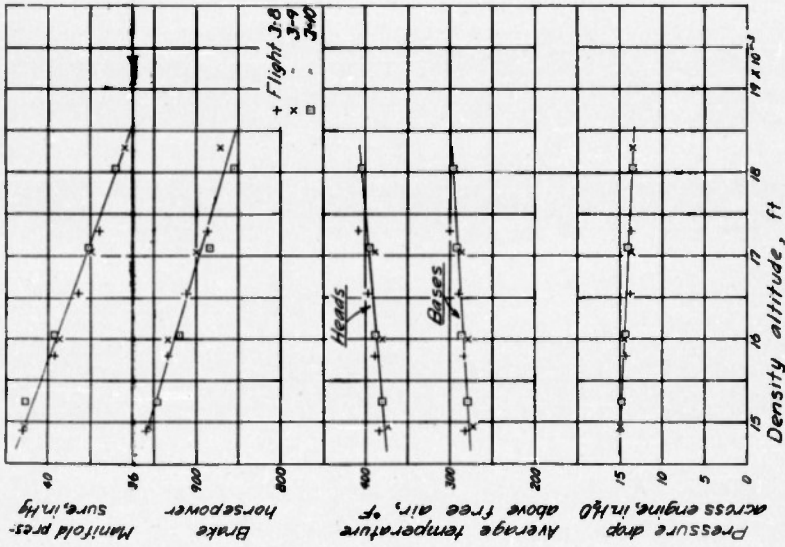


Fig 31

Figure 31.-Cooling-air pressure distribution and cylinder temperature. Flight 3-10.

L-383



Measure with
1/8" of inch

Figure 35.- Effect of altitude on cooling.

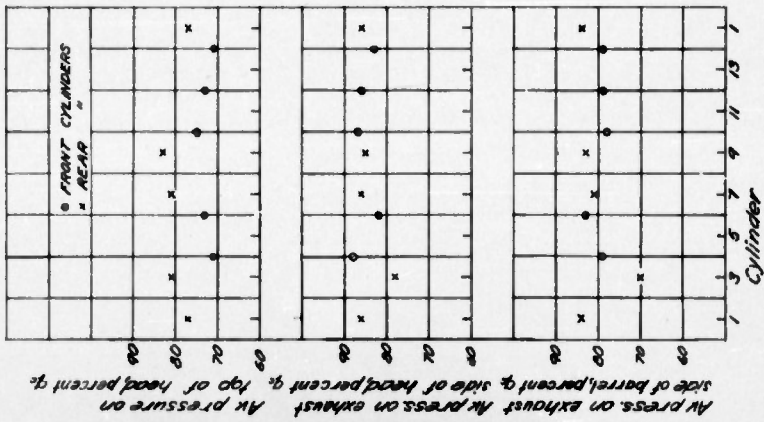


Figure 32.- Pressures at several locations on individual cylinders, averaged for all high-speed runs.

NACA

Figs. 34, 35

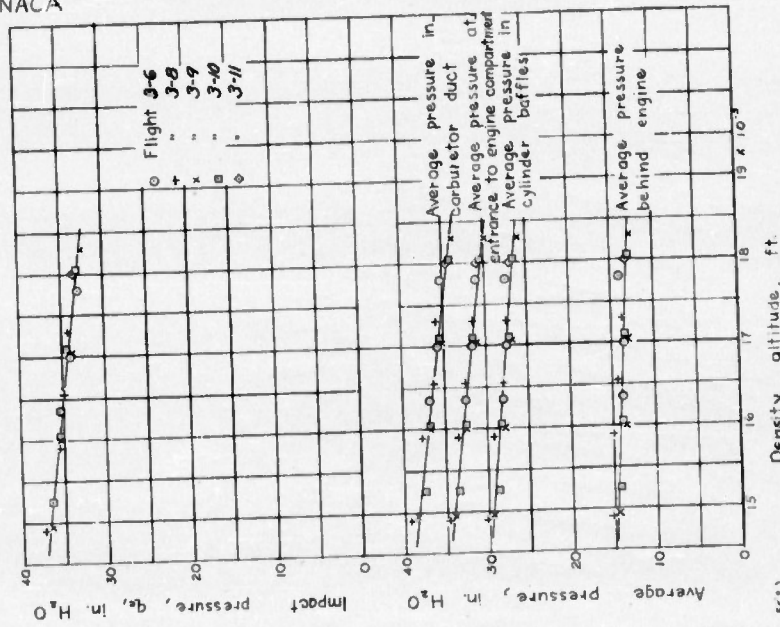


Figure 35.- Comparison of average induction and cooling-air pressures at several locations.

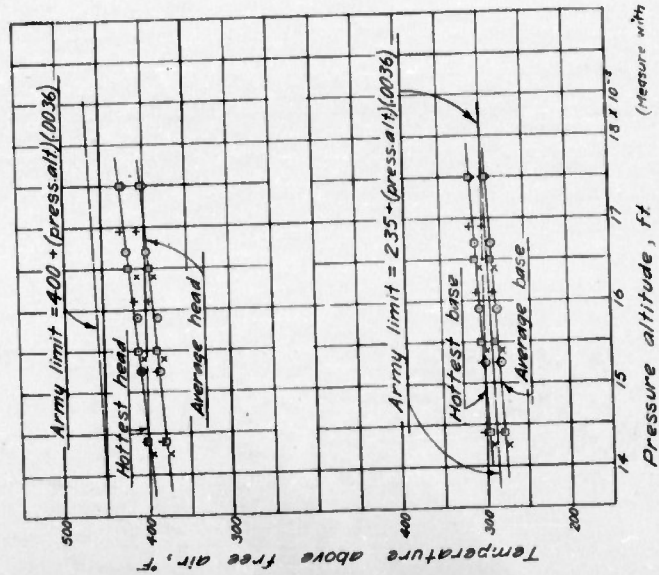


Figure 34.- Comparison of cylinder temperature with Army limits.

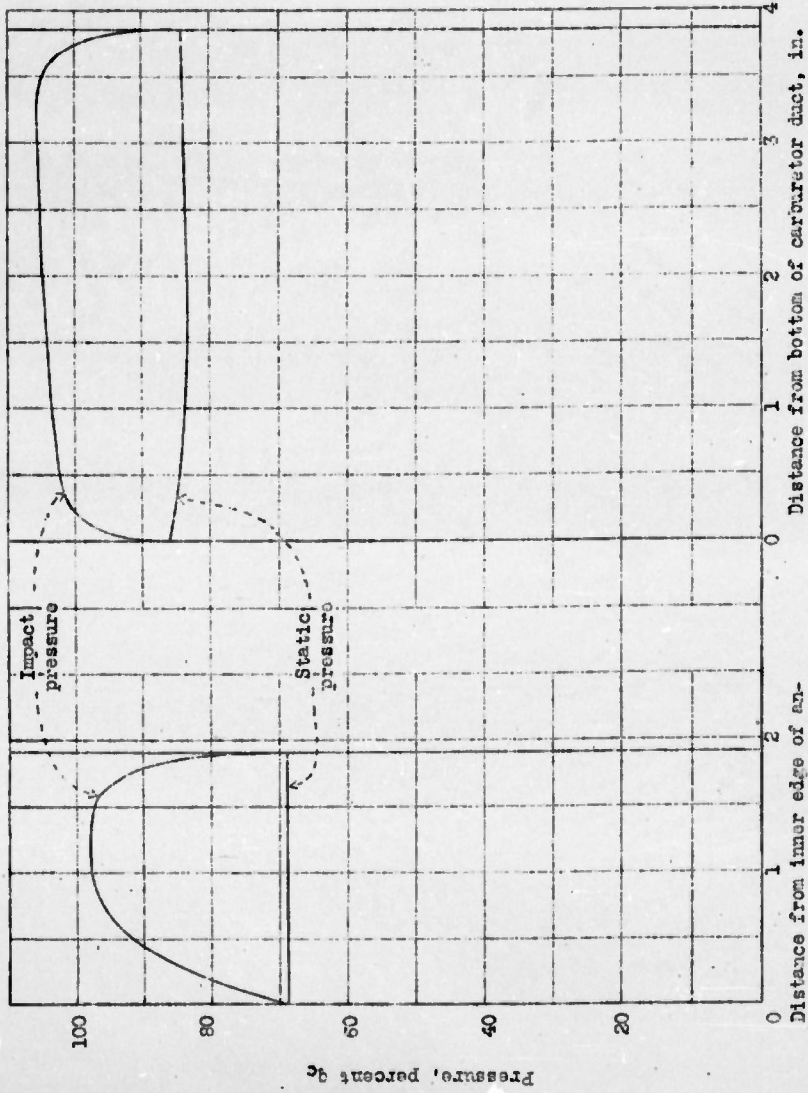


Fig. 36

Figure 36.- Average pressure distribution in annular entrance to engine compartment and in carburetor duct.

REEL - C

1 3 2

A.T.I.

5 5 3 6

TITLE: Flight Investigation of NACA DS Cowlings on the XP-42 Airplane - I - High Inlet Velocity Cowling with Propeller Cuffs Tested in High-speed Level Flight
AUTHOR(S): Bailey, F. J.; Johnston, J. F.
ORIGINATING AGENCY: National Advisory Committee for Aeronautics, Washington, D. C.
PUBLISHED BY: (Same)

ATI- 5536

REVISION
(none)

ORIG. AGENCY NO.
ARR-L-383

PUBLISHING AGENCY NO.
(none)

U

DATE	DOC. CLASS.	COUNTRY	LANGUAGE	PAGES	ILLUSTRATIONS
Jan '43	Unclass.	U.S.	Eng.	49	photos, tables, diagr, graphs

ABSTRACT:

Flight tests were made of maximum speed and cooling characteristics of XP-42 airplane equipped with a special cowling. Cooling-air pressures varied for different points of measurement on the same cylinder. Results of tests indicated maximum speed of 336 mph at 980 hp at 15,000 ft. Cooling-air pressure recovery on front of engine averaged 80% and rear pressure 39% of free steam-impact pressure.

Aircraft Engine Cowlings

P43

DISTRIBUTION: Request copies of this report only from Originating Agency

DIVISION: Power Plants, Reciprocating (6) 27
SECTION: Cooling (1) 14

SUBJECT HEADINGS: Cowlings, Engine (28005); Engines - Cooling tests (32882) XP-42 (28005)

ATI SHEET NO.: R-6-1-26

TITLE: Investigation of Maximum Error
AUTHOR(S): Estey, G. R.; Tesche, J.
ORIGINATING AGENCY: Consolidate
PUBLISHED BY: (Same)

DATE	DOC. CLASS.	COUNTRY
Nov '48	Secr.	U. S.

ABSTRACT:

The errors involved in the Mx-774 supersonic missile ground radars is caused by automatic propagation errors ground stations are isosce stalls. This system is

DISTRIBUTION: Copies of this report 1

DIVISION: Guided Missiles (1)
SECTION: Guidance and Control (1)

ATI SHEET NO.: S-1-1-83

Air Documents Division, Intelligence Department
Air Materiel Command

TITLE: Flight Investigation of NACA DS Cowlings on the XP-42 Airplane - I - High Inlet Velocity Cowling with Propeller Cuffs Tested in High-speed Level Flight
AUTHOR(S): Bailey, F. J.; Johnston, J. F.
ORIGINATING AGENCY: National Advisory Committee for Aeronautics, Washington, D. C.
PUBLISHED BY: (Same)

DATE	DOC. CLASS.	COUNTRY	LANGUAGE	PAGES	ILLUSTRATIONS
Jan '48	Unclass.	U.S.	Eng.	49	photos, tables, diagr, graphs

ABSTRACT:

Flight tests were made of maximum speed and cooling characteristics of XP-42 airplane equipped with a special cowling. Cooling-air pressures varied for different points of measurement on the same cylinder. Results of tests indicated maximum speed of 338 mph at 960 hp at 15,000 ft. Cooling-air pressure recovery on front of engine averaged 80% and rear pressure 39% of free stream-impact pressure.

DISTRIBUTION: Request copies of this report only from Originating Agency

DIVISION: Power Plants, Reciprocating (8)
SECTION: Cooling (1)

SUBJECT HEADINGS: Cowlings, Engine (28005); Engines - Cooling tests (32862) XP-42 (28005)

ATI SHEET NO.: R-8-1-28

Air Documents Division, Intelligence Department
Air Materiel Command

AIR TECHNICAL INDEX

Wright-Patterson Air Force Base
Dayton, Ohio

ATI- 5536

REVISION
(none)

ORIG. AGENCY NO.
ARR-L-383

PUBLISHING AGENCY NO.
(none)